

The Effects of Ground Water, Slope
Stability, and Seismic Hazard on
the Stability of the South Fork Castle
Creek Blockage in the Mount St. Helens
Area, Washington

U.S. GEOLOGICAL SURVEY PROFESSIONAL PAPER 1345



The Effects of Ground Water, Slope Stability, and Seismic Hazard on the Stability of the South Fork Castle Creek Blockage in the Mount St. Helens Area, Washington

By WILLIAM MEYER, M. A. SABOL, H. X. GLICKEN, *and* BARRY VOIGHT

U.S. GEOLOGICAL SURVEY PROFESSIONAL PAPER 1345



DEPARTMENT OF THE INTERIOR

DONALD PAUL HODEL, *Secretary*

U.S. GEOLOGICAL SURVEY

Dallas L. Peck, *Director*

Library of Congress Cataloging in Publication Data

Main entry under title:

The effects of ground water, slope stability, and seismic hazard on the stability of the South Fork Castle Creek blockage in the Mount St. Helens Area, Washington.

(Geological Survey professional paper ; 1345)

Bibliography: p. 41

Supt. of Docs. no.: I 19.16:1345

1. Landslides—Washington (State)—Castle Creek, South Fork. 2. Slopes (Soil mechanics) — Washington (State)—Castle Creek, South Fork. 3. Saint Helens, Mount (Wash.)—Eruption, 1980. I. Meyer, William, 1939— .II. Series.

QE599.U5E34 1985 551.3'53'0979784 84-600260

For sale by the Distribution Branch, U.S. Geological Survey
604 South Pickett Street, Alexandria, VA 22304

CONTENTS

	Page		Page
Abstract	1	Ground-water conditions	20
Introduction	1	Static slope-stability analysis	20
Acknowledgments	2	Modeled cross sections and assumptions	20
General description of the South Fork Castle Creek blockage	2	Results of static slope-stability analysis	24
Geologic setting	9	Retrogressive failure analysis	25
Preeruption geology	9	Seismic hazard	31
Posteruption geology	9	Seismic history of the blockage	35
Debris-avalanche deposit	12	Dynamic slope-stability analysis	35
Modern dacite, andesite, and basalt unit	12	Modeled cross sections and assumptions	35
Ancestral dacite unit	12	Calculation of n_s	35
Blast pyroclastic-flow deposits	12	Results of dynamic slope-stability analysis	37
Physical properties of blockage material	13	Displacement of sliding masses	38
Texture	13	Conclusions	40
Unit weight and relative density	13	References	41
Strength	15		

ILLUSTRATIONS

		Page
FIGURES	1-6. Maps showing:	
	1. Location of the study area and the Mount St. Helens seismic zone	3
	2. Preeruption topography of the study area, prepared by the Weyerhaeuser Company in 1950	4
	3. Posteruption topography of the South Fork Castle Creek blockage	5
	4. Thickness of the South Fork Castle Creek blockage	6
	5. Chronological appearance of slope-failure scarps on the South Fork Castle Creek blockage, as determined from aerial photography	7
	6. Geomorphic features mapped at South Fork Castle Creek blockage on September 22, 1982	8
	7. Stereopair of aerial photographs taken of South Fork Castle Creek blockage on September 22, 1982, showing slope-failure detachment scarp formed of multiple crescents	9
	8. Map showing the geology of the study area	10
	9. Photograph showing a typical exposure of blockage material	11
10, 11.	Graphs showing:	
	10. Results of direct shear-strength tests on the modern dacite, andesite, and basalt unit of the South Fork Castle Creek blockage: <i>A</i> , peak (maximum) strength; <i>B</i> , ultimate strength	16
	11. Results of direct shear-strength tests on the ancestral dacite unit of the avalanche debris from various sites: <i>A</i> , peak (maximum) strength; <i>B</i> , ultimate strength	18
12.	Map showing water-level contours for South Fork Castle Creek blockage, September 20, 1983	21
13.	Hydrographs for two selected piezometers at Coldwater Creek blockage	22
14.	Map showing location of cross sections on South Fork Castle Creek blockage that were analyzed for slope stability	23
15.	Diagram showing geology and September 1983 water levels at <i>A</i> , cross section AA'; <i>B</i> , cross section BB'; <i>C</i> , cross sections CD, CE, and CF; and <i>D</i> , cross section GG'	26
16.	Graphs showing variation of factor-of-safety values (F_s) versus seismic coefficients (n_s) for selected water levels at all cross sections	28
17-21.	Diagrams showing:	
	17. Critical failure surfaces predicted for <i>A</i> , cross section BB', and <i>B</i> , cross section GG', with water table at land surface and zero cohesion	30
	18. Critical failure surface and potential failure surface encompassing the largest section of the blockage for cross sections CE and CF with water table 25 ft above September 1983 levels and zero cohesion	31
	19. Critical failure surfaces predicted for cross section AA' with water table at land surface and <i>A</i> , 200 lb/ft ² cohesion and <i>B</i> , zero cohesion	32
	20. Critical failure surface and potential failure surface encompassing the largest section of the blockage for cross sections CE and CF with water table at land surface and <i>A</i> , zero cohesion and <i>B</i> , 200 lb/ft ² cohesion	33
	21. Predicted results of retrogressive slope-failure analysis on cross sections CD and CF with September 1983 water levels plus 25 ft and zero cohesion	34

	Page
FIGURES 22, 23. Diagrams showing:	
22. Predicted results of retrogressive slope-failure analysis on cross sections CD and CF with water table at land surface and zero cohesion	36
23. Critical surfaces and potential failure surfaces encompassing the largest sections of the blockage for cross sections CD, CE, and CF with a seismic coefficient of 0.2 g, September 1983 water level, and zero cohesion	39
24. Graph showing estimated displacement in the blockage resulting from an earthquake with an acceleration pulse of 0.5 g and duration of 0.1 and 0.2 seconds	40
25. Schematic of deformation expected with high ground-water level and maximum credible earthquake magnitude	41

TABLES

	Page
TABLE 1. Particle-size distribution in the South Fork Castle Creek blockage	13
2. Physical properties of the South Fork Castle Creek blockage and other sites on the debris-avalanche deposit	14
3. Model-predicted factors of safety (F_s^*) for critical failure surfaces at South Fork Castle Creek blockage for selected positions of the water table and cohesion values	24
4. Model-predicted factors of safety (F_s) for selected seismic coefficients (n_s)	38
5. Estimated displacement of sliding masses for selected positions of the water table at South Fork Castle Creek blockage	39

CONVERSION FACTORS AND ABBREVIATIONS

<i>Multiply</i>	<i>By</i>	<i>To obtain</i>
inches (in.)	25.4	millimeters (mm)
	2.540	centimeters (cm)
	0.0254	meters (m)
feet (ft)	0.3048	meters (m)
miles (mi)	1.609	kilometers (km)
square feet (ft ²)	0.09294	square meters (m ²)
square miles (mi ²)	2.590	square kilometers (km ²)
cubic feet (ft ³)	0.02832	cubic meters (m ³)
acre-feet (acre-ft)	1,233.0	cubic meters (m ³)
	0.001233	cubic hectometers (hm ³)
gallons per minute (gal/min)	0.06309	liters per second (L/s)
gallons per day (gal/d)	3.785	liters per day (L/d)
million gallons per day (Mgal/d)	3,785.0	cubic meters per day (m ³ /d)
feet per second (ft/s)	0.3048	meters per second (m/s)
pounds (lb)	0.4536	kilograms (kg)
pounds per cubic foot (lb/ft ³)	16.02	kilograms per cubic meter (kg/m ³)
Tons, short, per square foot (ton/ft ²)	9,765.0	kilograms per square meter (kg/m ²)
millimeters (mm)	0.03937	inches (in.)
centimeters (cm)	0.3937	inches (in.)

acceleration of gravity (g) = 32 feet per second squared, or 980.665 centimeters per second squared

National Geodetic Vertical Datum of 1929 (NGVD of 1929): A geodetic datum derived from a general adjustment of the first-order level nets of both the United States and Canada, formerly called mean sea level. NGVD of 1929 is referred to as a sea level in this report.

Tallany, Van Kuren, Gertis, and Thielman Datum of 1981 (TVGT of 1981): Datum derived from reference marks and surveyed at 1-mile intervals by TVGT and from auxiliary elevation control points surveyed by SPAN International, Inc. Specified accuracies were third order for reference marks and to 3 feet for auxiliary points.

THE EFFECTS OF GROUND WATER, SLOPE STABILITY, AND SEISMIC HAZARD ON THE STABILITY OF THE SOUTH FORK CASTLE CREEK BLOCKAGE IN THE MOUNT ST. HELENS AREA, WASHINGTON

By WILLIAM MEYER, M. A. SABOL,
H. X. GLICKEN, and BARRY VOIGHT

ABSTRACT

South Fork Castle Creek was blocked by the debris avalanche that occurred during the May 18, 1980, eruption of Mount St. Helens, Washington. A lake formed behind the blockage, eventually reaching a volume of approximately 19,000 acre-feet prior to construction of a spillway—a volume sufficiently large to pose a flood hazard of unknown magnitude to downstream areas if the lake were to break out as a result of blockage failure. Breakout of lakes formed in similar fashion is fairly common; breakouts in several places around the world have posed hazards in recent times.

The South Fork Castle Creek blockage consists of poorly sorted, unconsolidated deposits ranging from clay- and silt-sized particles to large blocks tens of feet across, and has a matrix of predominantly sand and gravel particles. Slopes on the blockage range from about 10 to 41 percent. Physical properties determined from field and laboratory tests suggest that the blockage debris is moderately compact and is probably typical of the debris avalanche.

In September 1983 a ground-water mound, 22 feet above lake level, caused flow from the mound to the lake and toward South Castle Creek. Depth to water below the crest to the blockage ranged from 20 to 60 feet. Ground-water levels are expected to fluctuate seasonally and may continue to increase annually until equilibrium is reached. September 1983 water levels are thought to be at their seasonal low and are expected to fluctuate by approximately 15 feet annually.

Analyses of blockage stability included determining the effects of gravitational forces and of horizontal forces induced by earthquakes of credible magnitude from the Mount St. Helens seismic zone, which passes within several miles of the blockage. The blockage is stable at September 1983 water levels under static gravitational forces. If an earthquake with magnitude near 6.0 local Richter level occurred with September 1983 water levels, movement on the order of 5 feet on both upstream and downstream parts of the blockage over much of its length could occur. If the sliding blocks liquefied, retrogressive failure could lead to lake breakout, but this is not considered probable.

As ground-water levels increase in the blockage above September 1983 levels, the overall possibility of slope failure on the blockage induced by gravitational and earthquake forces is increased. None of the analyses indicated that initial slope failure on the blockage would result in immediate lake breakout. Retrogressive slope failures could continue to lower the blockage, but lake breakout would occur only if liquefaction

of the sliding masses occurred during retrogressive failure, which is considered unlikely. The possibility of lake breakout as a result of slope failure induced on the blockage by gravitational or earthquake forces is therefore considered to be remote.

The most unstable conditions occur when the blockage is assumed to be saturated. A 50-foot rise in ground-water levels would saturate most of the blockage, in which case an earthquake near 6.0 in magnitude could cause movement of at least several tens of feet on both the upstream and downstream parts of the entire blockage. Factors of safety for slope failure induced by gravitational forces are less than 1.0 over several sections of the blockage when it is fully saturated.

INTRODUCTION

South Fork Castle Creek is a perennial stream that drains an area of 1.3 mi² on the northwest flank of Mount St. Helens. The creek was dammed by a debris avalanche that occurred during the May 18, 1980, eruption of Mount St. Helens. (The debris material is referred to in this report as the South Fork Castle Creek blockage or, simply, as the blockage.) A lake began forming directly behind the blockage and attained a volume of 19,000 acre-ft before a spillway constructed through the southeastern edge of the blockage in October 1981 stabilized its level. The volume of water in the lake (now known as South Fork Castle Creek Lake) is believed to be great enough to pose a flood hazard of unknown magnitude to downstream areas if the blockage should fail. The blockage could fail because of (1) slope failure induced by gravitational or earthquake forces, (2) liquefaction, (3) piping, and (or) (4) erosion.

This report contains the findings of a study aimed at estimating the possibility of slope failure in the blockage due to gravitational forces and earthquake-induced horizontal forces, and the effect on these forces of ground-water levels. The scope of the study included determining blockage thickness, mapping the geologic units in the blockage,

determining the material properties of the units, determining ground-water levels in the blockage, and, finally, using a digital model to estimate the potential for slope failure in the blockage due to static gravitational or earthquake forces.

It is fairly common for lakes to form as the result of emplacement of volcanoclastic debris across stream valleys during explosive volcanic eruptions, as is their subsequent breakout following failure or overtopping of their blockages. Stratigraphic studies by K. M. Scott and R. J. Janda, (written commun., 1983) indicate that prehistoric lahars resulting from the breakout of large lakes occurred many times at Mount St. Helens. In modern times, lake breakouts resulting from the failure or overtopping of dams of volcanoclastic debris occurred at Bandai-san Volcano in Japan in 1888 (Knott and Smith, 1890), Katmai Volcano in Alaska in 1912 or 1913 (Hildreth, 1983), and El Chichon Volcano in Mexico in 1982 (Silva and others, 1982).

The techniques used to analyze the stability of the South Fork Castle Creek blockage should be useful in determining the stability of existing dams of volcanoclastic debris and of those that may be emplaced by future explosive volcanic eruptions. In addition, the techniques should be applicable in studies of the stability of dams composed of suddenly emplaced, unconsolidated material from other large mass movements not associated with volcanic eruption. The dams formed by the Madison Canyon rockslide of 1959 in Montana (Hadley, 1978), the lower Gros Ventre slide of 1925 in Wyoming (Voight, 1978), the Mayunmarca rockslide of 1974 in Peru (Kojan and Hutchison, 1978), and the Nevados Huascaran avalanche of 1971 in Peru (Plafker and Ericksen, 1978) are examples of such nonvolcanic large mass movements.

ACKNOWLEDGMENTS

We thank the many people, both within and outside the U.S. Geological Survey, who helped with the analysis of the stability of the South Fork Castle Creek blockage. Robert Schuster, T. Leslie Youd, and William Smith of the USGS provided technical guidance in the initial evaluation of potential hazard at the blockage and assistance throughout the project. Craig S. Weaver, geophysicist, USGS, and Stephen D. Malone, senior research assistant, University of Washington, aided in obtaining information on the seismic history of the study area and the potential for earthquakes to affect the stability of the blockage. The U.S. Army Corps of Engineers extended their cooperation; specifically, Duane Bankofier and Stephen Loren Stockton provided data and pertinent information and Timothy J. Seeman did laboratory work on material properties. Finally, Sunil Sharma of Purdue University provided guidance in the use of the STABL3 slope-stability model.

GENERAL DESCRIPTION OF THE SOUTH FORK CASTLE CREEK BLOCKAGE

Prior to the May 18, 1980, eruption, South Fork Castle Creek entered Castle Creek about 6 mi from the summit of Mount St. Helens. Material from the debris avalanche blocked South Fork Castle Creek at its junction with Castle Creek, creating South Fork Castle Creek Lake. Castle Creek flowed along the south side of the valley of the North Fork Toutle River and was a tributary of the North Fork Toutle River (fig. 1), joining it 2.2 mi northwest of the site of the blockage.

In its September 1983 condition, South Fork Castle Creek Lake has a surface area of 480 acres, an average depth of 90 ft, and a volume of 19,000 acre-ft. The lake level has been stabilized at an elevation of 2,577 ft by a spillway.

The material blocking the lake comprises poorly sorted unconsolidated deposits, from clay- and silt-sized particles to large rocks many tens of feet across and some wood debris. The blockage is about 2,000 ft long from ridge to ridge and is about 1,400 ft wide, on the average, from the lake to the downstream toe. The maximum height of the blockage from the crest to the downstream toe is 190 ft, and from the crest to the lake 95 ft; vertical distance from the crest to the lake averages 60 ft. The altitude of the crest of the blockage ranges from 2,670 ft on the western side to 2,590 ft on the eastern side. Slopes average 28 percent from the crest of the blockage to the lake and range from 10 to 41 percent from the crest toward the Toutle River. The steepest slopes are on the western half of the blockage.

The thickness of the blockage was estimated by comparing preeruption and posteruption topography of the blockage area, using a 1:4800 topographic map prepared by the Weyerhouser Company in 1950 (fig. 2) and one prepared under contract with the USGS in 1981 (fig. 3), respectively. Comparison of stream and ridge locations on the two maps indicates a problem with horizontal control for at least one of the maps and suggests that the blockage thickness shown (fig. 4) for any point could be in error by an amount greater than the 10-foot contour interval—perhaps as great as 100 ft in areas of steep relief.

Some instances of mass movement have occurred on the blockage, but to date they have all been relatively small compared with the volume of the blockage. Twenty-one slope-failure scarps were mapped on the blockage using aerial photographs taken between May, 1980 and March, 1982 (figs. 5, 6). Additional features mapped on figure 6 include associated earthflow and debris-flow deposits; areas of standing water; fluvial surfaces (areas of running water or fluvial deposits); disturbed areas (roadways and other areas affected by construction of the spillway in the fall of 1981); and remnants of the original surface of the debris avalanche

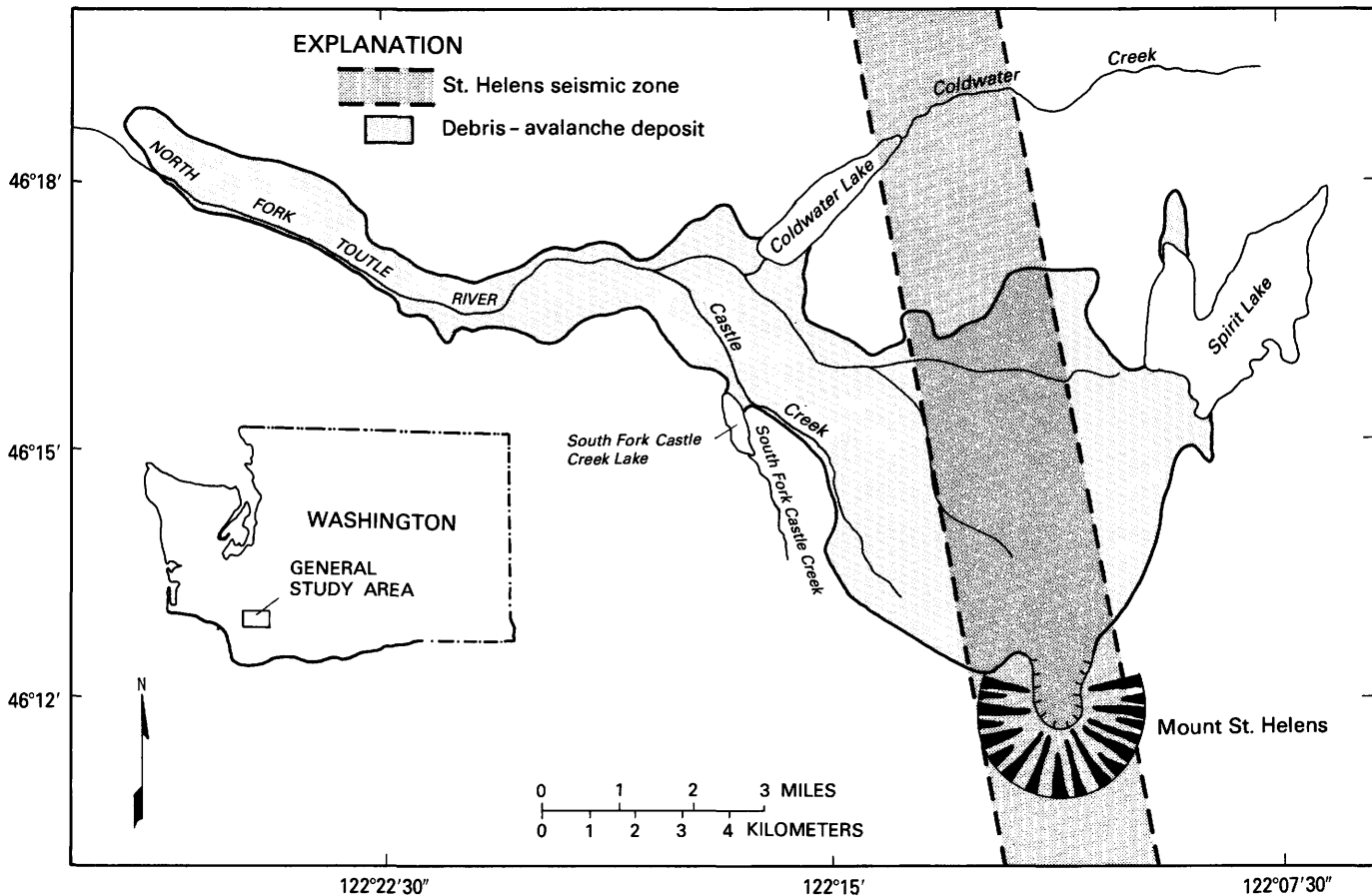


FIGURE 1.—Location of the study area and the Mount St. Helens seismic zone.

that are relatively unaffected by human activities, water, or secondary mass movements. Using the classification of Varnes (1978), the slope failures include debris slumps; slides along a concave-upward rupture surface; and debris slides, where movement of material occurs along relatively planar detachment surfaces. The rims of the larger scarps are often formed by multiple smaller crescent-shaped scarps, as shown in figure 7, and therefore individual scarps mapped on figures 5 and 6 do not always represent a single mass movement. There is no evidence, from either the sequential aerial photographs or field observations, of continued retrogressive failure.

To better understand the processes that might contribute to weakening of the blockage, the approximate dates of appearance of slope-failure scarps were determined from aerial photographs taken at selected times between May 18, 1980, and March 6, 1982 (fig. 5). The first three failures occurred in locally steep areas of the blockage between May 18 and November 12, 1980. Fourteen more failures occurred between November 12, 1980, and March 1, 1981. Four failures occurred between March 1, 1981, and March 6, 1982. None of the failures encompassed large areas of the blockage. The

failures that occurred between May 18, 1980, and March 1, 1981, are believed to have resulted mainly from a combination of locally oversteep relief and surface saturation from precipitation during the first period of winter rains following emplacement of the avalanche. The nearby Elk Lake earthquake that occurred on February 14, 1981, may have contributed to some of the failures, but this involvement cannot be documented. The final four scarps plotted are located along the bank of Castle Creek, suggesting that undercutting of the stream banks may have contributed to the instability. Were Castle Creek to migrate toward the blockage, erosion could change blockage geometry to the point that the blockage became unstable. This possibility is considered remote, but the morphology of the channel is nevertheless frequently monitored by aerial photography and by repeated cross-sectional surveys.

In general, mass movements on the blockage to date have occurred in areas where the topographic gradient was high; by smoothing the relief of the blockage such mass movements may have served to increase overall stability of the blockage. No surface manifestations of deep-seated instability are apparent.

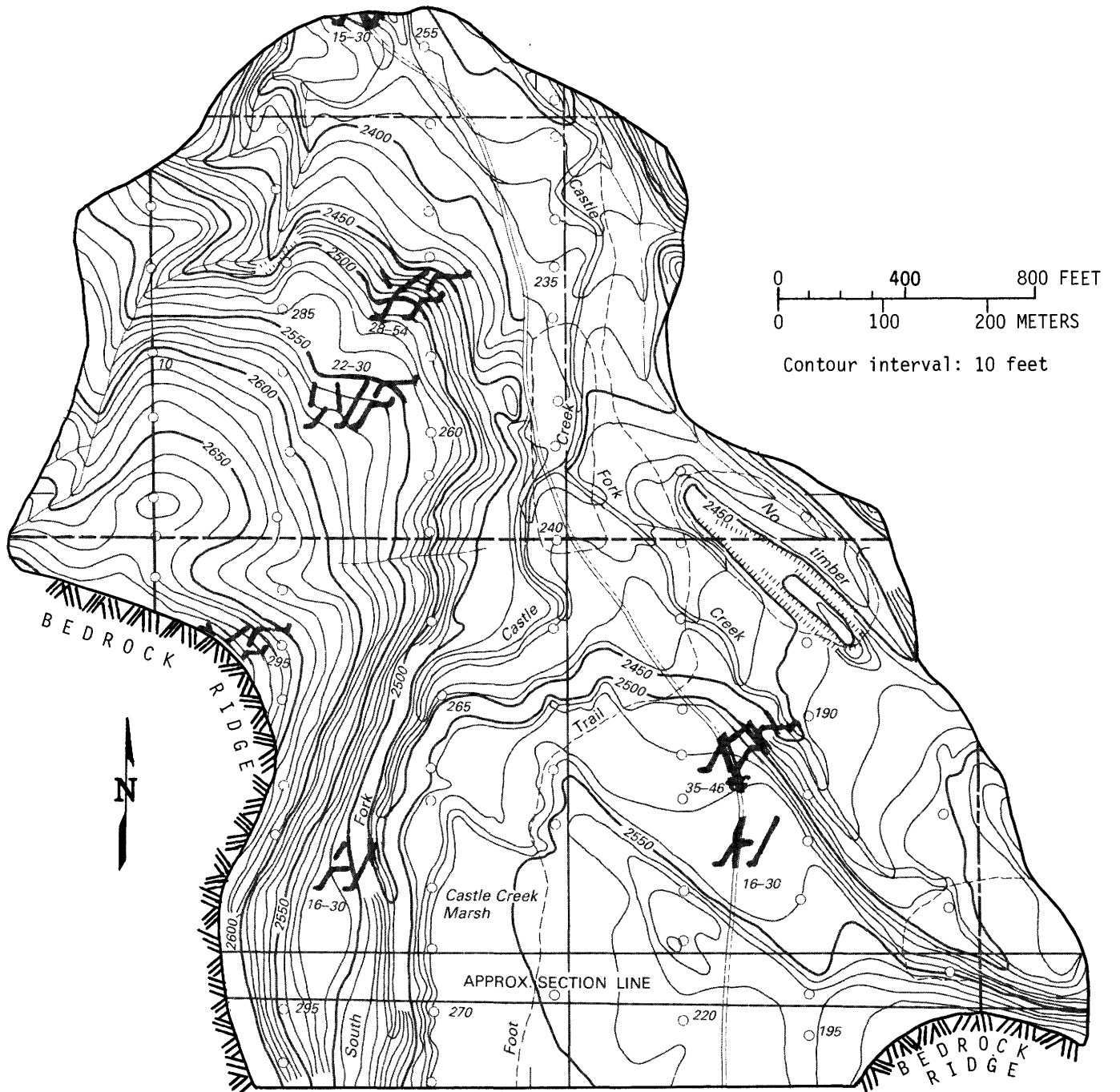


FIGURE 2.—Preeruption topography of the study area; map prepared by the Weyerhaeuser Company in 1950. Scale, 1:4800.

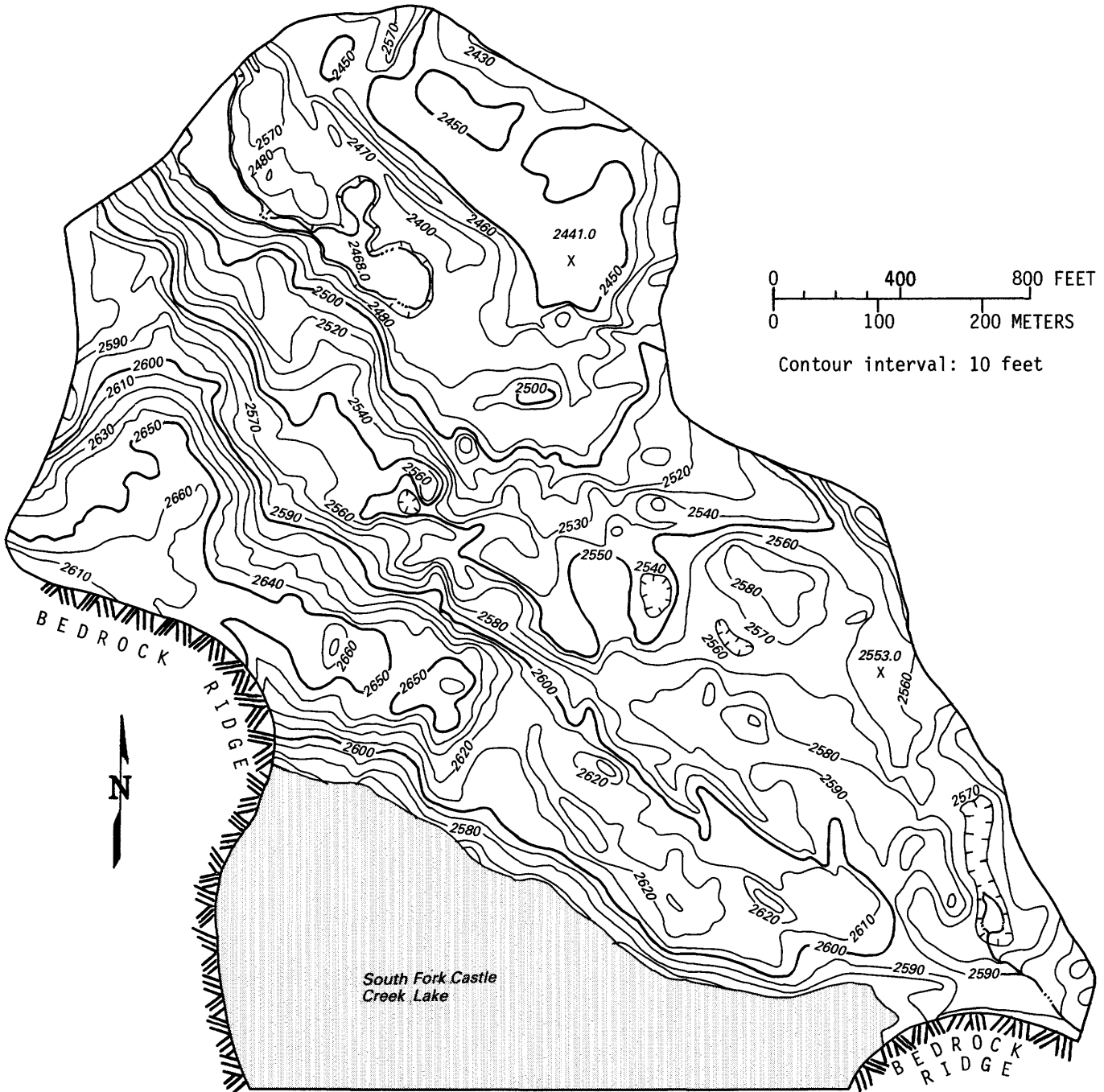


FIGURE 3.—Posteruption topography of the South Fork Castle Creek blockage.

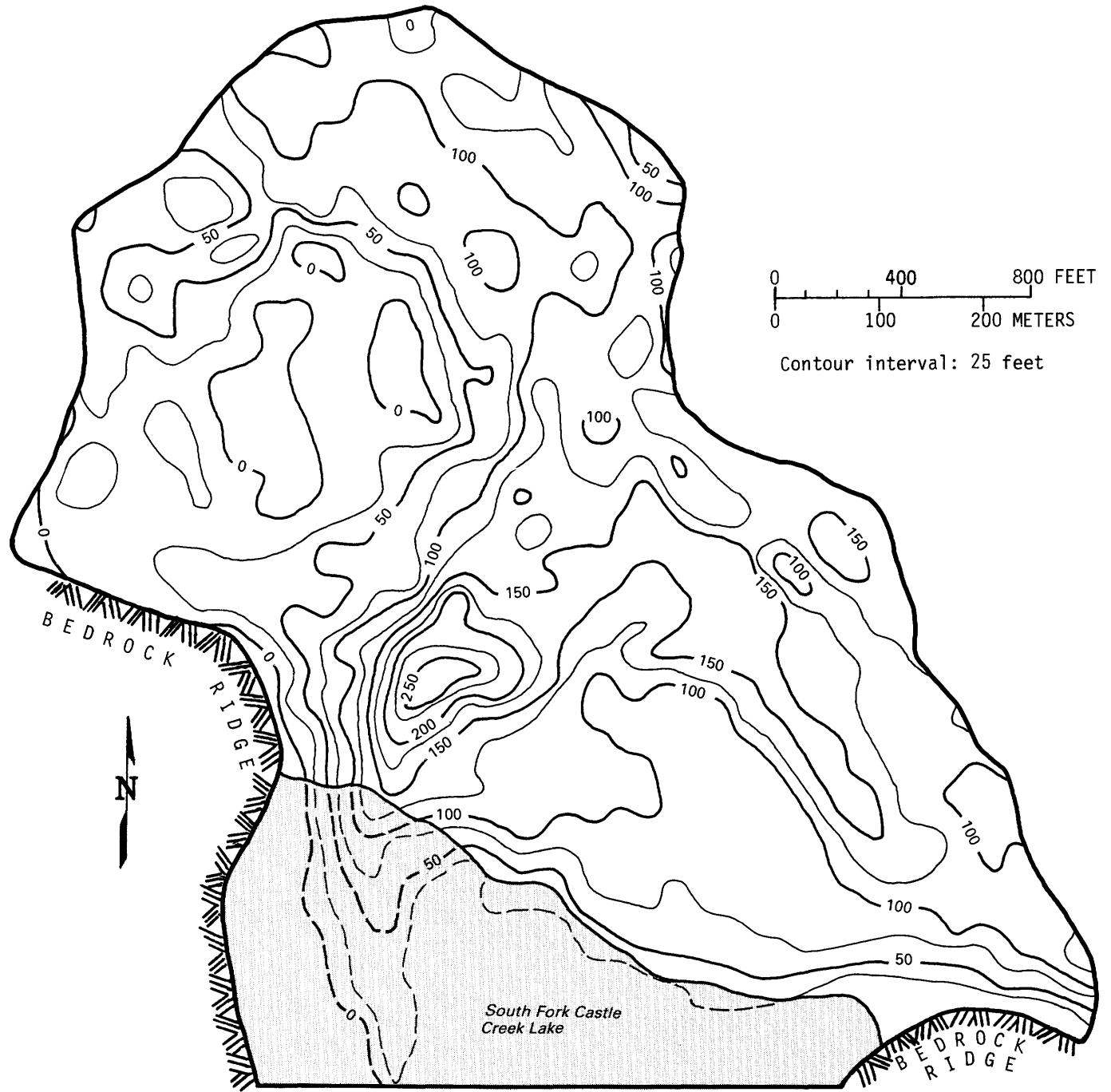


FIGURE 4.—Thickness of the South Fork Castle Creek blockage.

EXPLANATION

- Contact
- - - Inferred

Designation	Slope-failure between:
A	5/18/80 and 6/19/80
B	6/20/80 and 11/12/80
C	11/13/80 and 2/02/81
D	2/03/81 and 3/01/81
E	3/02/81 and 7/27/81
F	7/28/81 and 2/07/82
G	2/08/82 and 3/06/82

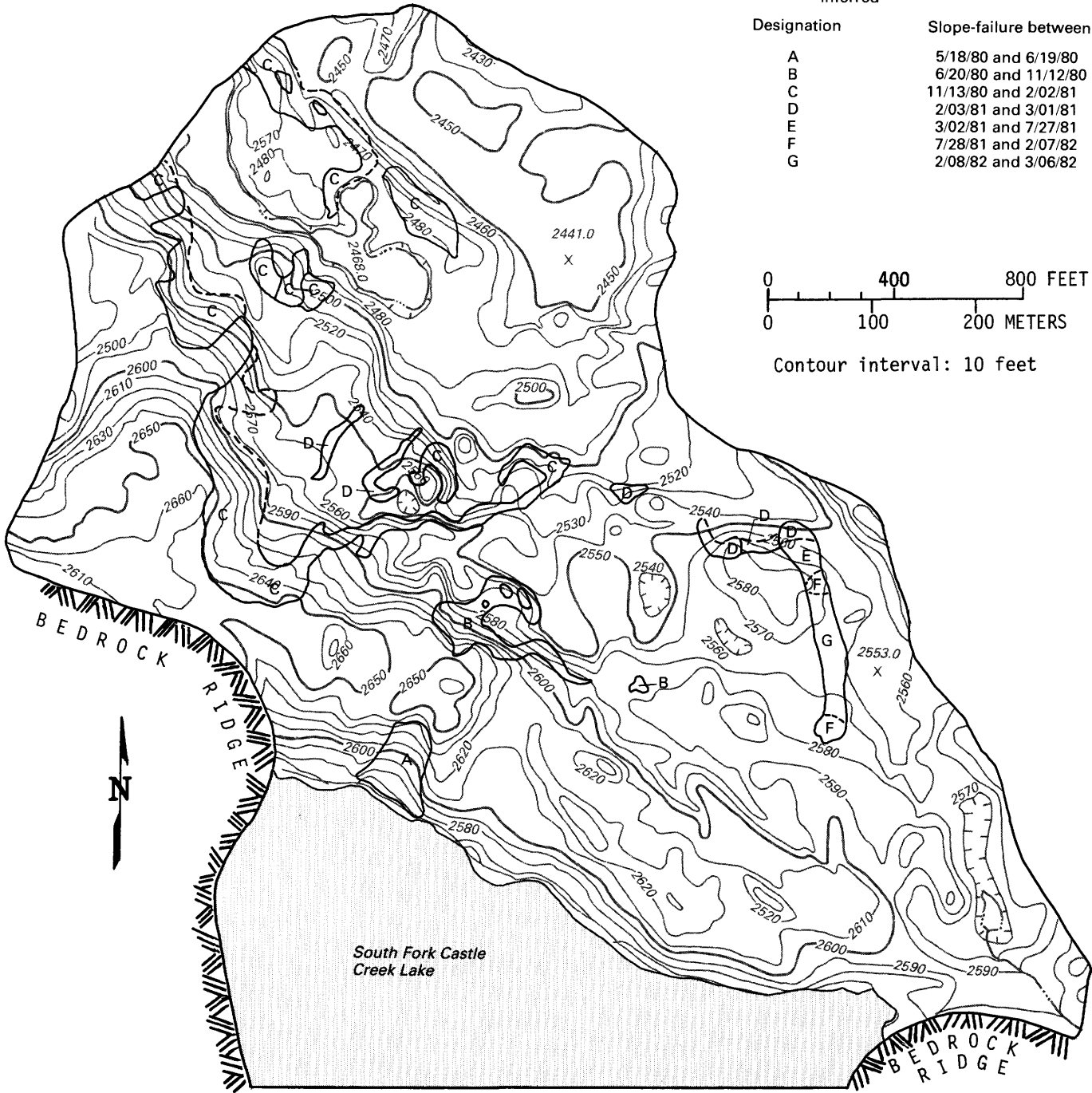
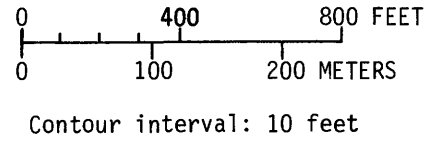
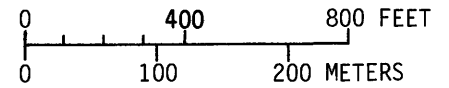


FIGURE 5.—Chronological appearance of slope-failure scarps on the South Fork Castle Creek blockage, as determined from aerial photography.

EXPLANATION

- W Standing water
- F Fluvial surfaces (running water or fluvial deposits)
- D Disturbed areas
- DS Earthflow or debris-flow deposits
- SF Slope-failure scarps
- O Original surface of blockage

- Contact
- - - Inferred contact



Contour interval: 10 feet

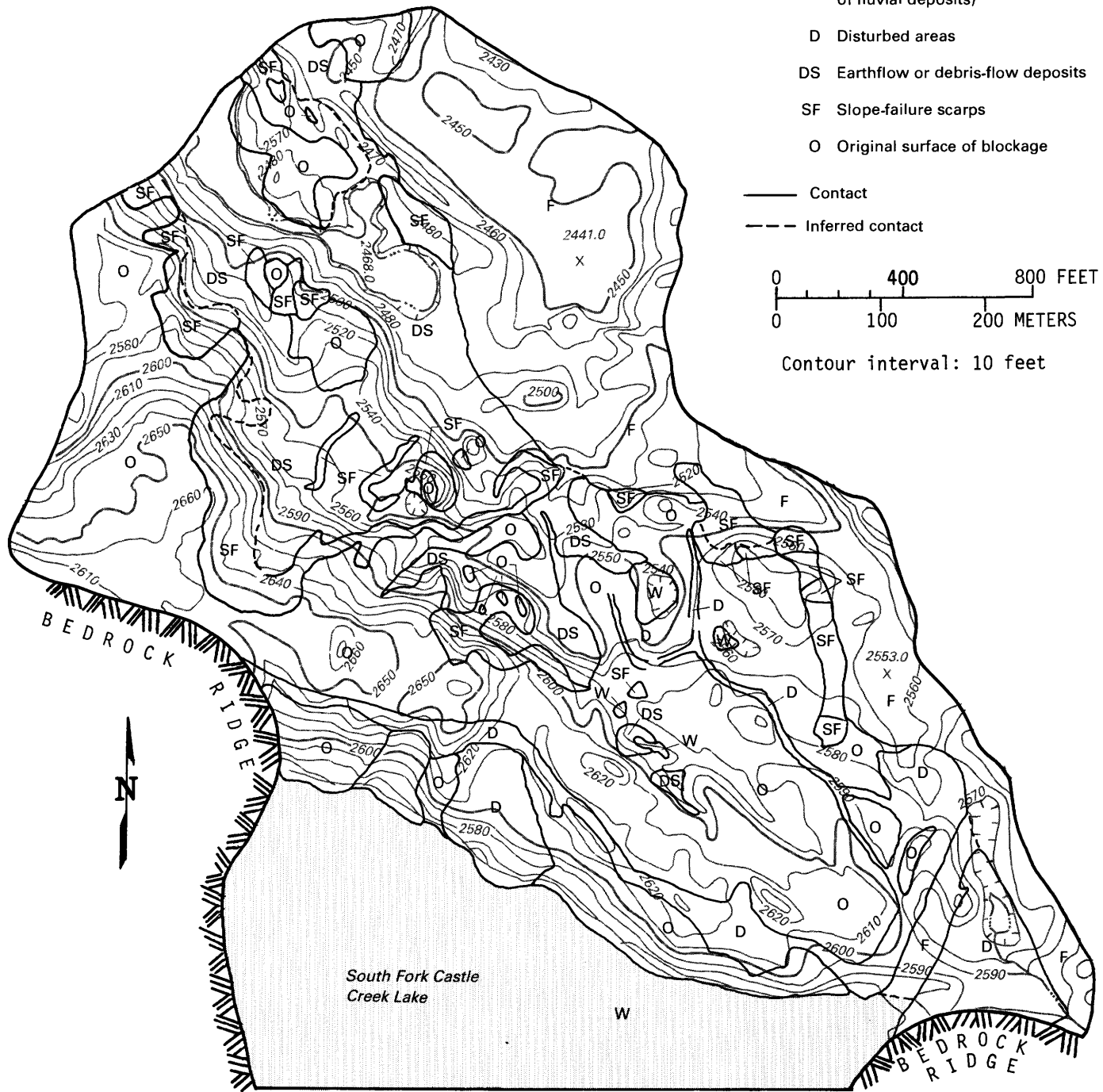


FIGURE 6.—Geomorphic features mapped at South Fork Castle Creek blockage on September 22, 1982.

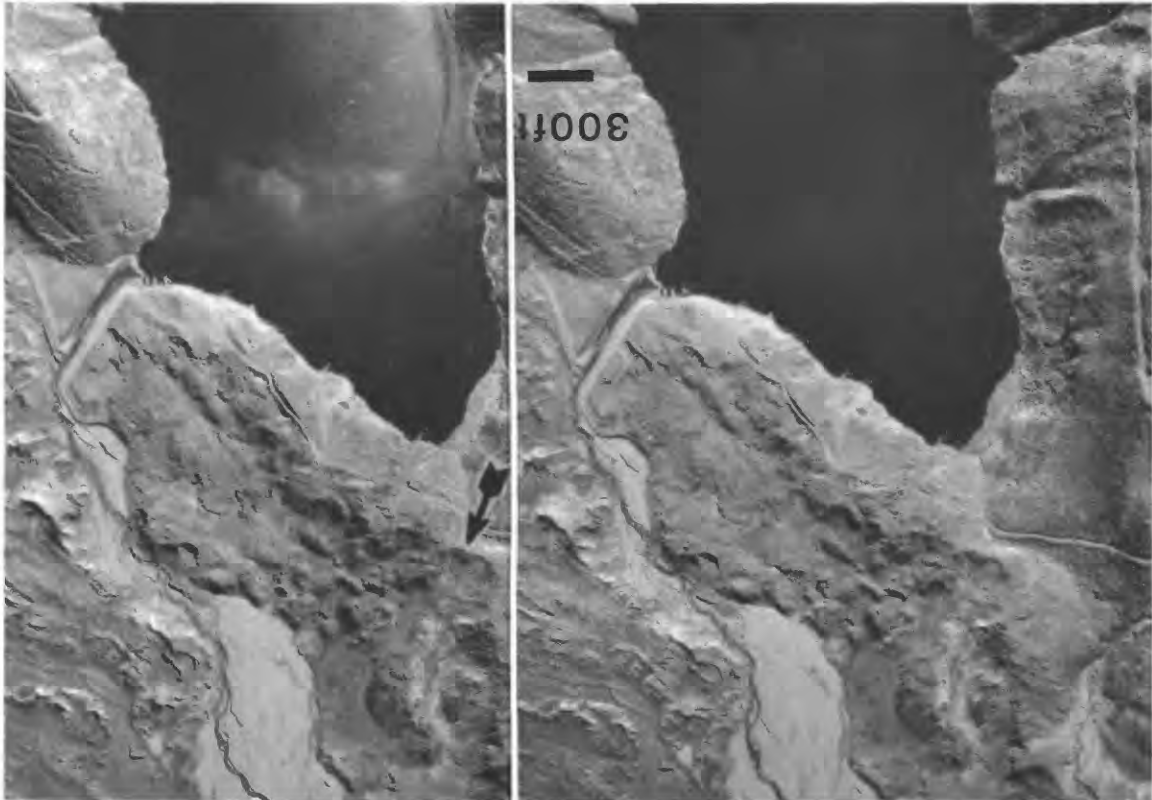


FIGURE 7.—Stereopair of aerial photographs taken of South Fork Castle Creek blockage on September 22, 1982, showing slope-failure detachment scarps (arrow) formed of multiple crescents.

GEOLOGIC SETTING PREFRUPTION GEOLOGY

Castle Creek was contained within a channel 130 ft deep into a broad northward-sloping fill of unconsolidated volcaniclastic debris from Mount St. Helens (fig. 2). This fill, of unknown thickness, is composed primarily of pyroclastic flows and lahars more than 2,500 years old. However, exposures along the canyon revealed unconsolidated deposits less than 180 years old and an augite-hypersthene andesite lava flow 2,200–2,500 years old (C. A. Hopson, written commun., 1983). A similar channel at the northern edge of the fill contained the North Fork Toutle River.

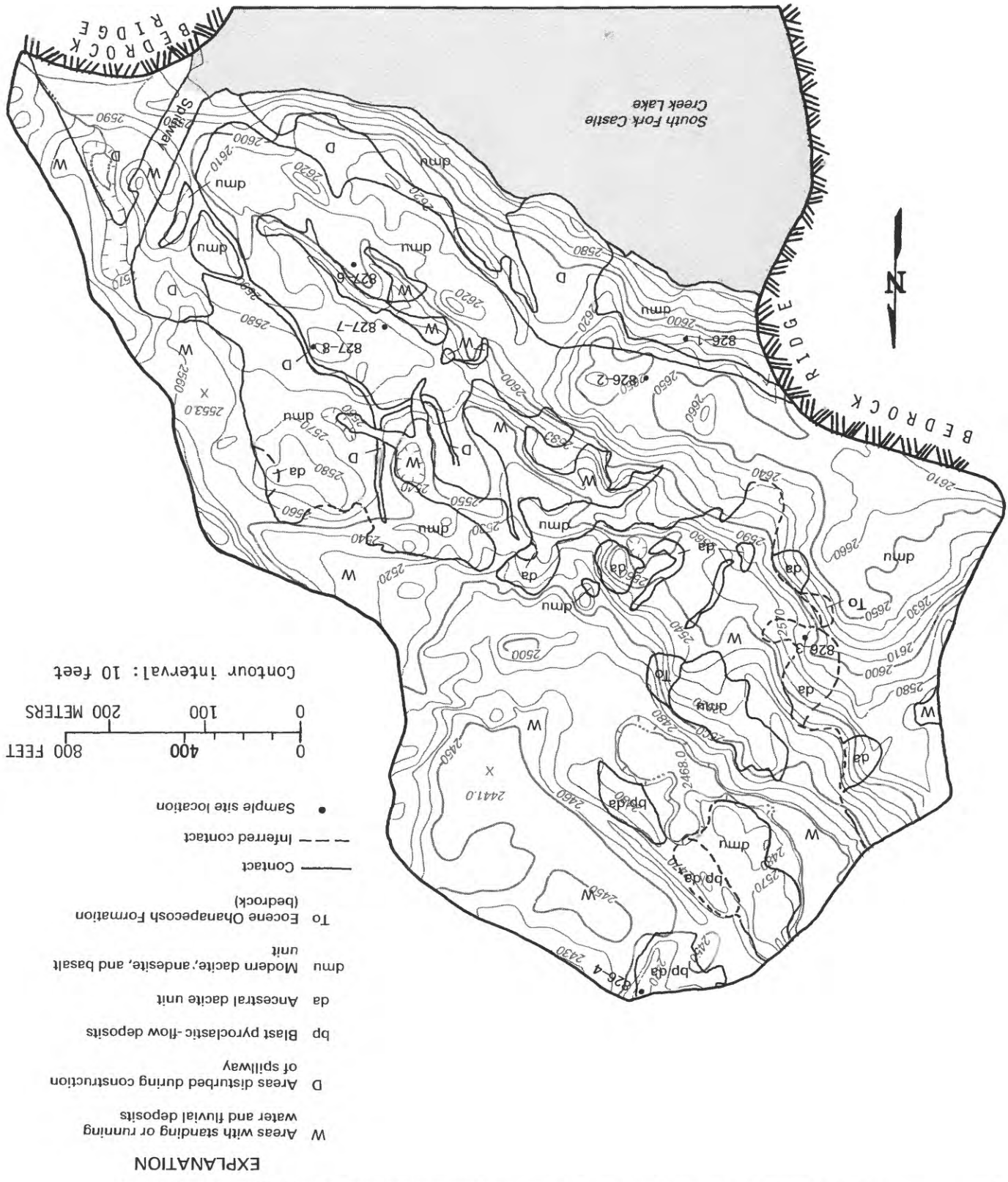
South Fork Castle Creek also flowed in a 130-foot-deep channel (fig. 2) cut into southward-sloping unconsolidated volcaniclastic deposits from Mount St. Helens more than 2,500 years old (C. A. Hopson, written commun., 1983). The thickness of these deposits is also unknown. Approximately 1,300 ft south of the conjunction of Castle Creek and South Fork Castle Creek was a swampy, flat, alluvium-filled area called Castle Creek Marsh (fig. 2). The southwesterly slope of the volcaniclastic material indicated that in prehistoric time thick pyroclastic flows or lahars from Mount St. Helens flowed up South Fork Castle Creek and probably blocked it, forming a lake at the site of Castle Creek Marsh. When the ancient lake filled, its waters probably overtopped the prehistoric blockage

and drained suddenly, in a manner similar to that of some of the smaller lakes on the 1980 debris-avalanche deposit (Jennings and others, 1981). If this scenario is correct, the channel of the pre-May 18, 1980, South Fork Castle Creek was cut at the time of the ancient lake breakout.

The valleys containing Castle Creek and South Fork Castle Creek are bounded by bedrock ridges of the Eocene or Early Oligocene Ohanapecos Formation. The Ohanapecos in this area consists of andesitic and dacitic volcanic rocks, both lava flows and breccias, and associated volcaniclastic sedimentary rocks. The Ohanapecos has undergone widespread low-temperature, low-pressure zeolite facies alteration (C. A. Hopson, written commun., 1983).

POSTERUPTION GEOLOGY

The South Fork Castle Creek blockage is composed almost entirely of the deposit of the debris avalanche of May 18, 1980 (figs. 8, 9), mapped and described by Voight and others (1981). The debris-avalanche deposit is overlain by blast pyroclastic-flow deposits (Lipman, 1981), generally less than 1 ft thick but in lower areas of the blockage more than 15 ft thick. Ash falling from the air during the eruptions of May 18, May 25, and August 7, 1980, is less than 1 in. thick at the blockage (Sarna-Wojcicki and others, 1981).



EXPLANATION

- W Areas with standing or running water and fluvial deposits
- D Areas disturbed during construction of spillway
- bp Blast pyroclastic-flow deposits
- da Ancestral dacite unit
- dmu Modern dacite, andesite, and basalt unit
- To Eocene Chanapacosh Formation (bedrock)
- Contact
- - - Inferred contact
- Sample site location

0 400 800 FEET
 0 100 200 METERS
 Contour interval: 10 feet

FIGURE 8.—Geology of the study area.



FIGURE 9.—A typical exposure of blockage material.

DEBRIS-AVALANCHE DEPOSIT

Voight and others (1981) indicated that the South Fork Castle Creek blockage is composed of lateral deposits (levee material) of the North Toutle unit of the debris-avalanche deposit. The units they mapped are identified primarily on the basis of unmodified morphologic characteristics. Because the blockage is composed of levee material, the slopes of the ridges and hummocks that make up the blockage are steeper than those of the bulk of the debris-avalanche deposit. The lithologic composition of the levee material is distinctly different from that of the bulk of the avalanche deposit.

The blockage consists of two major lithologic units that are informally referred to in this report as the ancestral dacite unit and the modern dacite, andesite, and basalt unit. In addition, a small area of blast pyroclastic-flow deposits that in places overlie ancestral dacite was mapped where the blast deposits are more than 5 ft thick (fig. 8). These units are described on the basis of field characteristics; detailed petrographic results are not included.

Modern Dacite, Andesite, and Basalt Unit

The modern dacite, andesite, and basalt unit (dmu on fig. 8) is an unsorted, mostly unstratified mixture of material ranging from silt-clay-sized particles to boulders up to 5 ft across. The rock types in the unit are predominantly dacite, andesite, and basalt from the modern (less than 2,500-year-old) cone of Mount St. Helens, as mapped by C. A. Hopson (written commun., 1983). (The distinction between the lavas of the modern cone and an underlying "old Mount St. Helens series" was noted by Verhoogen (1937). Hopson (written commun., 1983) referred to "modern" and "ancestral" lavas, and his terminology is adopted for this report.)

Minor amounts of ancestral dacite, dacitic pumice, and organic debris from the old mountain are also found in the modern dacite, andesite, and basalt unit, but the proportions are difficult to estimate because of the lack of good exposures. Examination of surficial float and selected outcrops cleared of slopewash suggests that dacite, andesite, and basalt from the modern cone of Mount St. Helens make up more than 75 percent of the unit.

The modern dacite must have come from the Goat Rocks or the Summit domes or from their volcanoclastic debris. These were the only dacite exposures on the Mount St. Helens edifice prior to May 18, 1980, and were the only two domes less than 2,500 years old that were incorporated in the debris avalanche (Voight and others, 1981). The Goat Rocks and Summit domes were composed of augite-hornblende-hypersthene dacite that is grey when fresh and various shades of red or pink when hydrothermally altered. The dacite is nearly aphyric in hand specimen, but close examination reveals micropheno-

crysts of hornblende, pyroxene, and plagioclase, generally less than 0.1 in. long. Xenoliths of varying composition are common in these and other domes of Mount St. Helens (Hopson, oral commun., 1980).

The modern andesite and basalt rocks within the debris-avalanche deposit are derived from various lava flows on the pre-1980 edifice of Mount St. Helens (Verhoogen, 1937; Hopson, written commun., 1983), indistinguishable in hand specimen. The rocks are generally black or dark grey but are locally various shades of green or red when hydrothermally altered. The andesite is generally plagioclase phyric with varying amounts of hypersthene and augite. Olivine is rare and usually occurs as phenocrysts less than 0.05 in. across. The basalt is either aphyric or olivine-phyric and is much less abundant than the andesite. The andesite and basalt range from nonvesicular to scoriaceous.

Ancestral Dacite Unit

The ancestral dacite unit (da on fig. 8) is an unsorted, unstratified mixture of material ranging from silt- and clay-sized particles to clasts many feet in diameter. Much more homogeneous than the modern dacite, andesite, and basalt unit, the ancestral dacite unit consists almost entirely of the "ancestral dacite" lithology, often hydrothermally altered. However, lenses of andesitic breccia, generally measuring less than 1 ft², are observed locally. These probably represent brecciated andesite dikes, created from dikes similar to the undeformed ones observed in the present crater of Mount St. Helens. Brecciated dikes may also be blended into the ancestral dacite; of 100 pebbles 1-4 in. in diameter that were examined at one exposure, 88 percent are ancestral dacite and 12 percent are other lithologies, primarily andesite.

The ancestral dacite originates from the complex of dacitic domes and associated breccias more than 2,500 years old that make up the core of Mount St. Helens. These rocks are present in the light-colored exposures in the 1980 crater below 7,500 ft, and they form a few exposed domes around the flanks of the mountain. The ancestral dacite lithology is readily identified in the field. It is a hornblende-hypersthene dacite, grey when fresh and various shades of red, pink, and green when hydrothermally altered. It contains prominent phenocrysts of hornblende and plagioclase greater than 0.1 in. long, as well as less prominent hypersthene phenocrysts. Xenoliths of varying composition are present locally.

BLAST PYROCLASTIC-FLOW DEPOSITS

The blast pyroclastic-flow deposits (bp on fig. 8) are the hot, highly fragmented deposits of the directed blast of May 18, 1980. They were mapped only in the northwest corner of the study area where they are more than 5 ft thick and overlie ancestral dacite.

TABLE 1.—Particle-size distribution in the South Fork Castle Creek blockage

Sample number	Geologic unit	Particle-size classification			Median diameter (millimeters)	Gradation	
		Gravel (percent)	Sand (percent)	Silt-clay (percent)		Uniformity coefficient ²	Sorting coefficient ³
82-826-1 --	dmu ¹	43.6	47.0	9.4	0.7	42	5
82-826-2 --	do.	54.9	37.3	7.8	1.3	42	6
82-827-8 --	do.	56.2	36.8	7.0	3.5	91	8
82-827-6 --	do.	48.9	40.7	10.4	1.7	74	8
82-827-7 --	do.	44.8	42.4	12.8	1.2	66	8
82-826-3 --	Ancestral dacite	41.8	49.0	9.2	1.1	37	6
82-826-4 --	Blast pyroclastic-flow deposit	33.1	50.9	16.0	0.5	25	6

¹Modern dacite, andesite, and basalt unit.

³Sorting coefficient of Trask (1930).

²Uniformity coefficient (Hazen's): ratio of the diameter at the 60-percent-finer point and that at the 10-percent-finer point on a gradation curve.

Where exposed, the blast pyroclastic-flow deposits are generally a poorly sorted, unstratified mixture of angular material ranging from silt- and clay-sized particles to fragments several inches in diameter. They are identified by an undulating, wavy upper surface and olive-grey exposures that contain a blended mix of all pre-1980 Mount St. Helens rock types. They contain a characteristic prismatic jointed, semivesicular steel-blue-grey hypersthene-hornblende dacite that is referred to as blast dacite and is thought to be juvenile material representing fragments of the pre-May 18, 1980, cryptodome (Hoblitt and others, 1981).

On the higher areas of the blockage, the blast pyroclastic-flow deposits generally are finer grained and do not contain clasts larger than half an inch in diameter. The unit here has characteristics similar to those of layers A2 and A3 of Waitt (1981) and of the pyroclastic surge and accretionary lapilli units of Hoblitt and others (1981).

PHYSICAL PROPERTIES OF BLOCKAGE MATERIAL

TEXTURE

Samples weighing from 4 to 11 lb were collected in the blockage material at five sites in the modern dacite, andesite, and basalt unit (which composes most the blockage) and at one site each in the ancestral dacite unit and the blast pyroclastic-flow deposits to determine particle-size distribution. Only particles less than 64 mm were considered in the analysis, although blocks meters in diameter are present locally. All the units are poorly sorted. Silt and clay content for the samples from the modern dacite, andesite, and basalt unit ranged from 7.0 to 12.8 percent, sand content from 36.8 to 47.0 percent, and gravel content from 43.6 to 56.2 percent. Corresponding values for the single sample

from the ancestral dacite unit were 9.2, 49.0, and 41.8 percent, and for the blast pyroclastic-flow deposit 16.0, 50.9, and 33.1 percent. Median diameters for the modern dacite, andesite, and basalt unit ranged from 0.7 to 3.5 mm; the sample median diameter for the ancestral dacite unit was 1.1 mm and for blast pyroclastic-flow deposits, 0.5 mm. Uniformity coefficients (table 1) ranged from 25 to 91; those values are lower than the average of 104 reported for the avalanche as a whole by Voight and others (1981).

Particle-size data alone provide an incomplete picture of the texture of the modern dacite, andesite, and basalt unit. When vertical exposures of at least 10 ft² are cleared of loose material, many lithologically distinct blocks of breccia from the old mountain in various degrees of disaggregation can be seen. A typical exposure is shown in figure 9. Although the material properties differ slightly from block to block, the range is probably reasonably represented by the sampling.

UNIT WEIGHT AND RELATIVE DENSITY

Physical properties of particles measuring less than 4.75 mm were determined for eight samples from the modern dacite, andesite, and basalt unit; one sample from the ancestral dacite unit; and one sample of blast pyroclastic-flow deposit from the blockage (table 2). Physical properties of samples from five sites on the debris avalanche outside the blockage are also shown for comparison.

True specific gravities of the modern dacite, andesite, and basalt unit samples just described ranged from 2.57 to 2.70 (table 2). The samples of the ancestral dacite and blast pyroclastic-flow units had specific gravities of 2.68 and 2.69, respectively.

Dry unit weight (γ_d), determined by the sand-cone method, gave values for the avalanche in the range of

TABLE 2.—Physical properties of the South Fork Castle Creek blockage and other sites on the debris-avalanche deposit

[Particle size less than or equal to 4.75 mm; γ_{\min} , laboratory-determined minimum unit weight, in pounds per cubic foot; γ_{\max} , laboratory-determined maximum unit weight, in pounds per cubic foot; D_r , relative density; c' , cohesion, in tons per square foot; θ' , effective friction angle; θ^* , apparent friction angle]

Sample number	Geologic unit	Specific gravity	Dry weight (lbs/ft ³)	Field water content (pct)	Void ratio ²	Porosity ² (pct)	γ_{\min} (lbs/ft ³)	γ_{\max} (lbs/ft ³)	γ_{D_r} (pct)	c' (ton/ft ²)	θ' (degree)	θ^* (degree)
South Fork Castle Creek Blockage:												
82-826-1	dmu ³	2.70	99.3	5.6	0.70	40	117.1	136.3	0	—	—	—
82-826-2	do.	2.70	94.3	3.0	.79	43	115.0	134.8	0	—	—	—
82-827-6	do.	2.57	89.9	8.2	.79	46	82.4	93.2	55	0.10	38	38.5
82-827-7	do.	2.60	93.6	9.3	.73	44	97.2	113.6	0	.25	35	36
82-827-8	do.	2.66	103.6	5.2	.53	34	113.0	132.4	0	.20	36	37
CC1 ⁴	do.	—	105.9	—	—	—	—	—	—	—	—	—
CC2 ⁴	do.	—	119.6	—	—	—	—	—	—	—	—	—
CC3 ⁴	do.	—	116.1	—	—	—	—	—	—	—	—	—
82-826-3	Ancestral dacite	2.68	90.5	3.4	.85	45	109.1	129.0	0	—	—	—
82-826-4	Blast pyroclastic flow	2.69	126.1	6.2	.33	24	136.7	127.6	93	.50	41.5	44
Debris avalanche, various sites:												
DX5-3	Modern dacite	2.69	115.4	—	—	—	95.5	117.0	95	.20	33.5	35
DX3-20	Ancestral dacite	2.71	129.8	—	—	—	108.2	137.3	26	.40	30	35
DX5-24	do.	2.75	116.1	—	—	—	85.2	112.6	100	0	35	35
COE	do.	2.73	130.0	*8.0	.31	24	108.1	132.6	91	2.14	36.9	52
COE	do.	2.73	118.9	—	.43	30	107.5	128.5	—	.23	44.9	45

¹Results for South Fork Castle Creek blockage samples are suspect, as noted in text.

²Calculations using average specific gravity, 2.65.

³Modern dacite, andesite, and basalt unit.

⁴L. Youd, R. Schuster, and B. Voight, U.S. Geological Survey, 1983.

⁵Assumed water content.

90 to 120 lb/ft³ (table 2). This wide range and the low average value of 102 lb/ft³ possibly reflects late and (or) postdepositional disturbances of portions of the blockage; materials in sheared or slumped levee walls and boundary zones have been observed locally to be less dense than less disturbed debris elsewhere on the avalanche (Voight and others, 1981). However, operator error is suspected in several of these measurements. Three measurements considered reliable give a range of 106 to 120 lb/ft³ and an average of 114 lb/ft³ (Youd, Schuster, and Voight, written commun., 1983). One sample of the blast pyroclastic-flow deposit yielded a dry unit weight of 126 lb/ft³.

Water content, w , the weight of water divided by the weight of dry solids and expressed as a percentage, ranged from 3.0 to 9.3 percent and averaged 6.9 percent. Because samples were obtained near the surface following a dry period in August 1982, these values may be low in comparison with representative material at depth.

Including unreliable samples, the calculated average wet unit weight (the product of $(1+w)$ and dry unit weight) for the South Fork Castle Creek blockage at the time of sampling was 109 lb/ft³. The average value of reliable measurements was 122 lb/ft³.

By comparison, wet-unit-weight measurements for four large samples (6 ft in diameter and several feet thick) from the debris-avalanche deposit near Spirit Lake averaged 120 lb/ft³ for an average water content of about 8.8 percent (three samples; T. J. Seeman, written commun., 1983). On the basis of these measurements, the average dry unit weight is 108 lb/ft³, a value somewhat less reliable than the wet weight because of assumptions made about water content. The average dry unit weight for 36 conventional sandcone measurements widely distributed over the avalanche is 119 lb/ft³ (H. X. Glicken, written commun., 1983). The more reliable data from the blockage, yielding an average dry unit weight of 114 lb/ft³, thus suggest that unit-weight values are similar to those at other sites on the debris-avalanche deposit.

Relative densities, D_r , (Terzaghi and Peck, 1967) were calculated by comparing field dry unit weights, γ_d , with laboratory-determined maximum and minimum unit weights, γ_{dmax} and d_{min} , and are reported as percentage:

$$D_r = \left(\frac{\gamma_d - d_{min}}{\gamma_{dmax} - \gamma_{dmin}} \right) \left(\frac{\gamma_{dmax}}{\gamma_d} \right) \cdot 100.$$

Laboratory tests were performed on samples from the blockage using material 3 in. or less in diameter in 0.5-cubic-foot cylindrical molds. Maximum unit weights

were determined using dry samples subjected to a 0.14-ton-per-square-foot surcharge on a vibratory table. Minimum unit weights were gained by gentle placement of debris into the mold, and the test was repeated until consistent results to within 1 percent were obtained.

For the samples from the South Fork Castle Creek blockage, relative density of the blast pyroclastic-flow deposit sample was 93 percent; relative density of one sample from the debris-deposit avalanche was 55 percent. For the remaining samples from the debris-avalanche deposit, relative density was less than 0 (that is, dry unit weight was less than minimum unit weight) (table 2). The result, $D_r < 0$, is probably caused by erroneous field determinations of dry unit weight. Laboratory determinations of dry densities are considered accurate (table 2); in these tests, average values of minimum and maximum dry unit weight for five samples from the modern dacite, andesite, and basalt unit were 105.1 and 122.9 lb/ft³, respectively. Using these as extreme values, the average field dry unit weight of 113.9 lb/ft³ for these samples (based on three measurements that were considered reliable) corresponds to a relative density of 53 percent. The average of 25 determinations of relative density distributed over the entire avalanche is 48 percent, a comparable value. Although fragmentary, the data suggest that the degree of compaction of the deposit at South Fork Castle Creek is probably typical of all avalanche debris.

STRENGTH

Laboratory-drained direct-shear tests were conducted at the North Pacific Division Material Laboratory, U.S. Army Corps of Engineers, Portland, Oreg., on representative splits of one sample from the blast pyroclastic-flow deposit and three samples from the modern dacite, andesite, and basalt unit (T. J. Seeman, written commun., 1983). The fraction of the samples less than 4.75 mm was compacted to approximately field density, as estimated by sandcone measurements in a shear box 3-in. square and 0.75 in. thick. A normal pressure of 3 tons/ft² was applied, and after a 24-hour soaking period, shearing was accomplished at a rate of 0.001 in. per minute to a displacement of 0.5 in. The procedure was repeated on fresh sample splits for normal pressures of 5 and 10 tons/ft².

The samples from the debris-avalanche deposit show slight development of peak strength and mainly contractive volumetric changes, characteristic of loose specimens of particulate material and in keeping with the low field estimates of dry unit weight. Linear Coulomb regressions for individual samples give effective stress-friction angles (ϕ') of 35° to 38° and cohesion intercepts (c') of from 0.10 to 0.25 ton/ft² (table 2). Forcing the Coulomb envelope through the origin gives apparent friction angles (ϕ^*) of

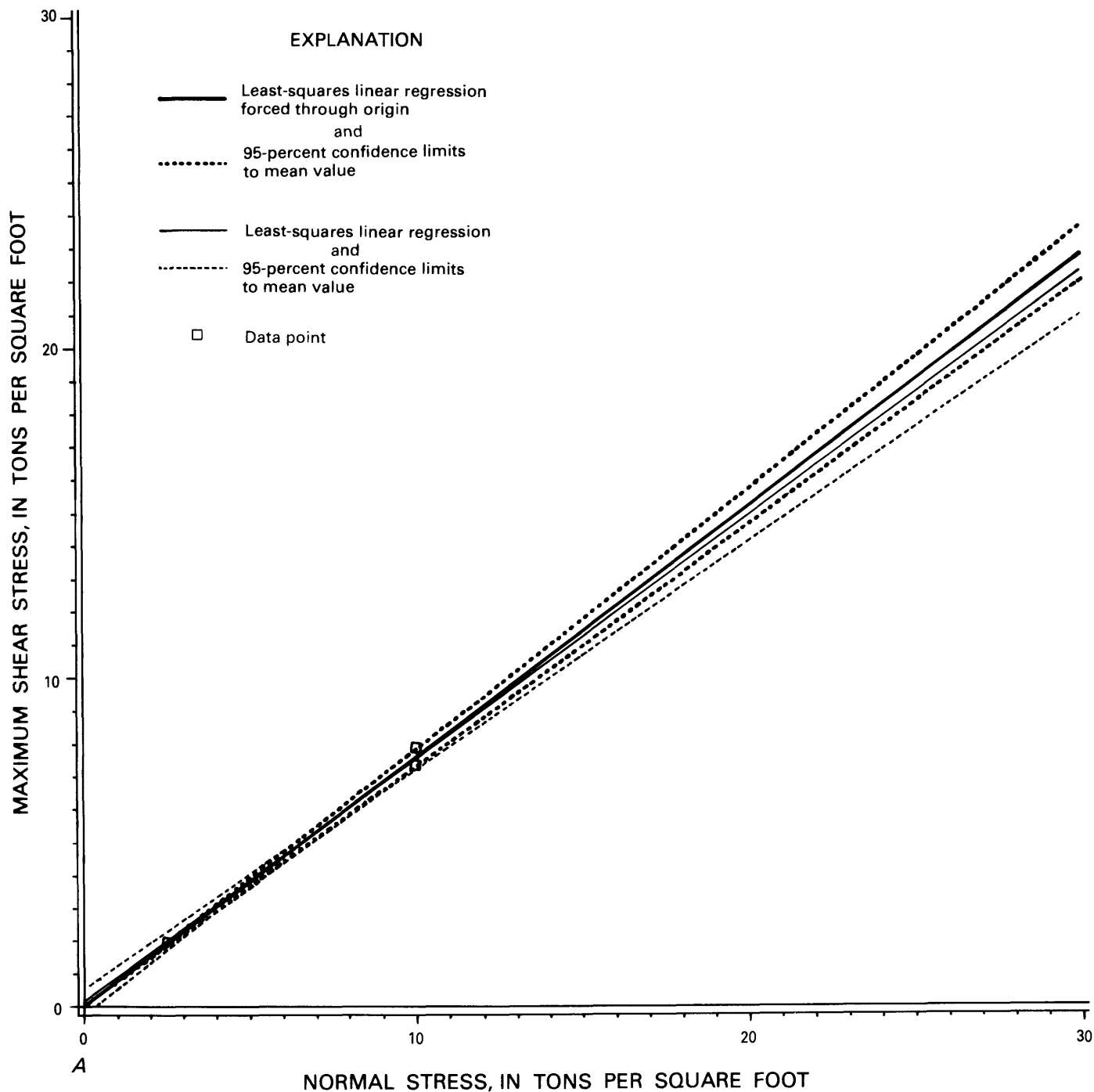


FIGURE 10.—Results of direct shear-strength tests on the modern dacite, andesite, and basalt unit of the South Fork Castle Creek blockage: A, peak (maximum) strength.

36° to 38.5° fitted through data points in the normal pressure range of 3 to 5 tons/ft² (table 2).

Combined data for samples from the modern dacite, andesite, and basalt unit yield, by least squares analysis,

an average intercept of 0.16 ton/ft² and peak ϕ' of 36.4° ($r^2=0.966$; fig. 10A). Also for combined data, peak ϕ^* is 37.1° ($r^2=0.999$) and ultimate ϕ^* is 34.9° ($r^2=0.999$; fig. 10B). The peak-strength estimates for these samples are

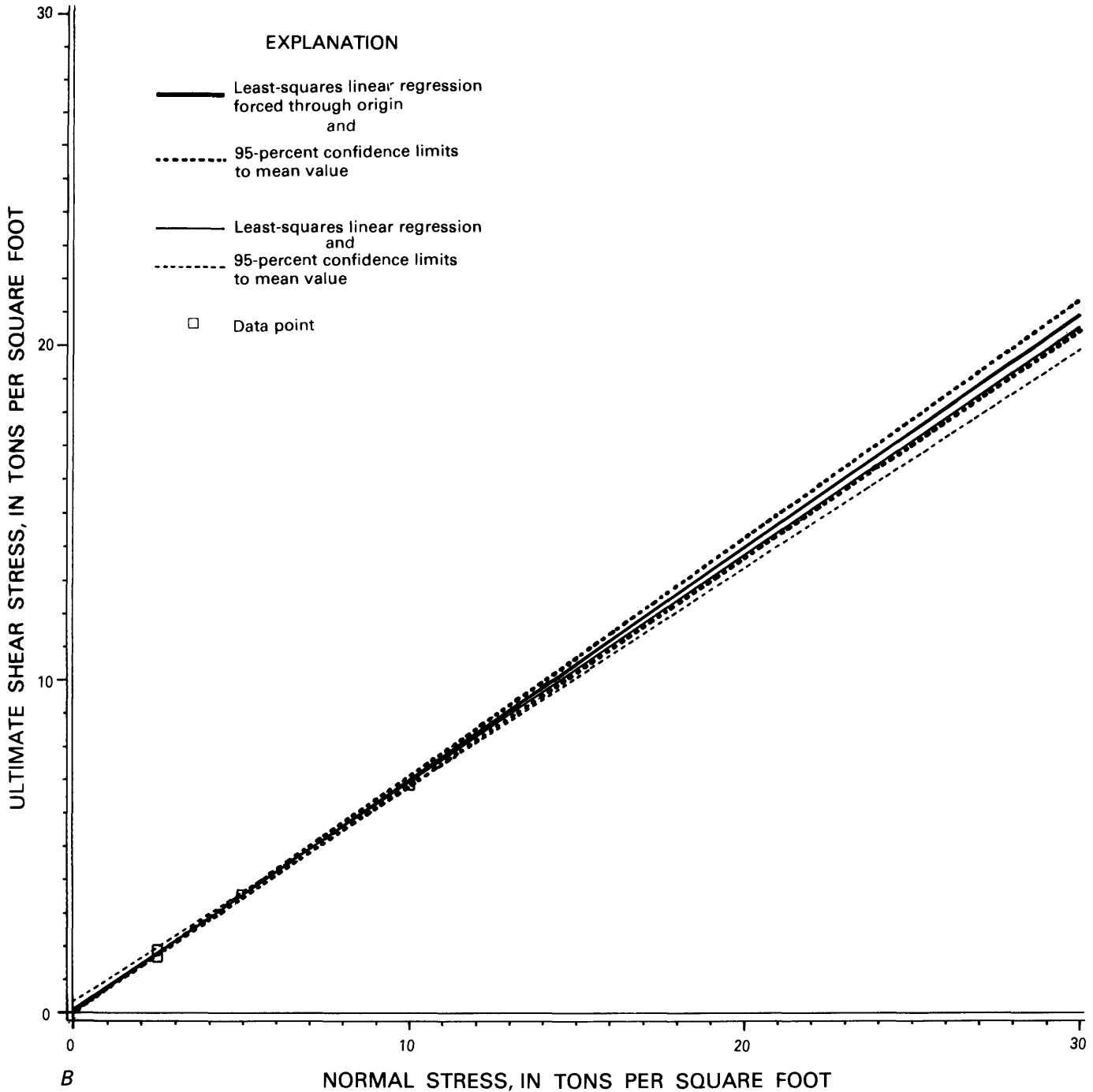


FIGURE 10.—Results of direct shear-strength tests on the modern dacite, andesite, and basalt unit of the South Fork Castle Creek blockage: *B*, ultimate strength.

conservative, because the strength tests were carried out at a degree of compaction believed to be small compared with the more reliable field estimates. A comparison sample, DXS-3, taken adjacent to the blockage from debris

composed mainly of modern dacite, gave comparable values (table 2).

The sample from the blast pyroclastic-flow deposit, with $D_r=93$, was stronger than the sample from the mod-

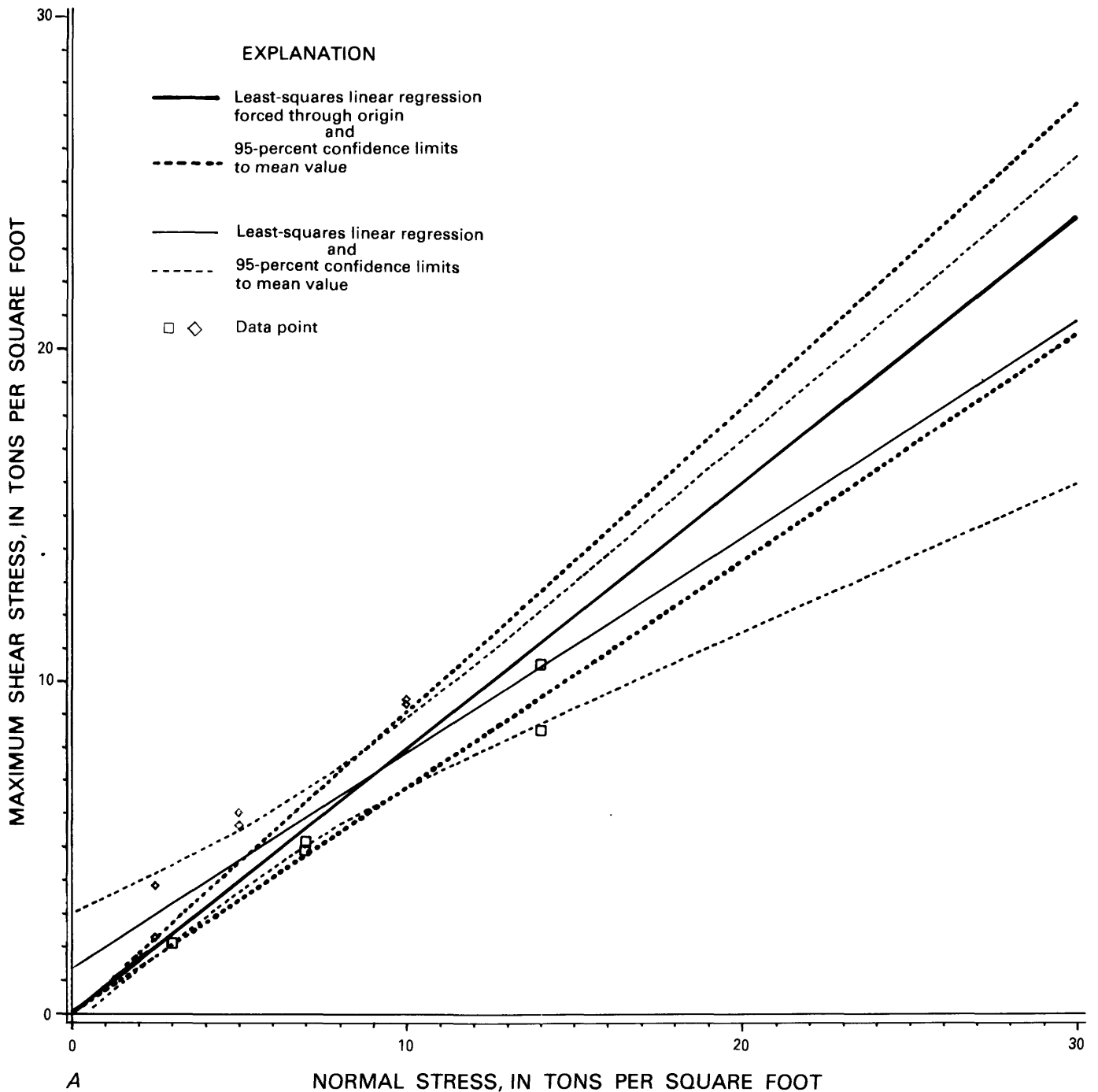


FIGURE 11.—Results of direct shear-strength tests on the ancestral dacite unit of the avalanche debris from various sites: A, peak (maximum) strength.

ern unit debris-avalanche sample, with $\phi' = 41.5^\circ$ and $c' = 0.50$ ton/ft², and peak $\phi^* = 44^\circ$. Combined results for five samples from the blast pyroclastic-flow deposit at various sites between Castle Creek and Spirit Lake (average $D_r = 61$) indicate peak $\phi' = 33.64^\circ$ and $c' = 1.42$ tons/

ft² ($r^2 = 0.721$); peak $\phi^* = 39^\circ$ ($r^2 = 0.932$), and ultimate $\phi^* = 33.6^\circ$ ($r^2 = 0.966$).

Strength determinations were not made for the ancestral dacite unit of the debris-avalanche deposit at South Fork Castle Creek, but the combined results for four sam-

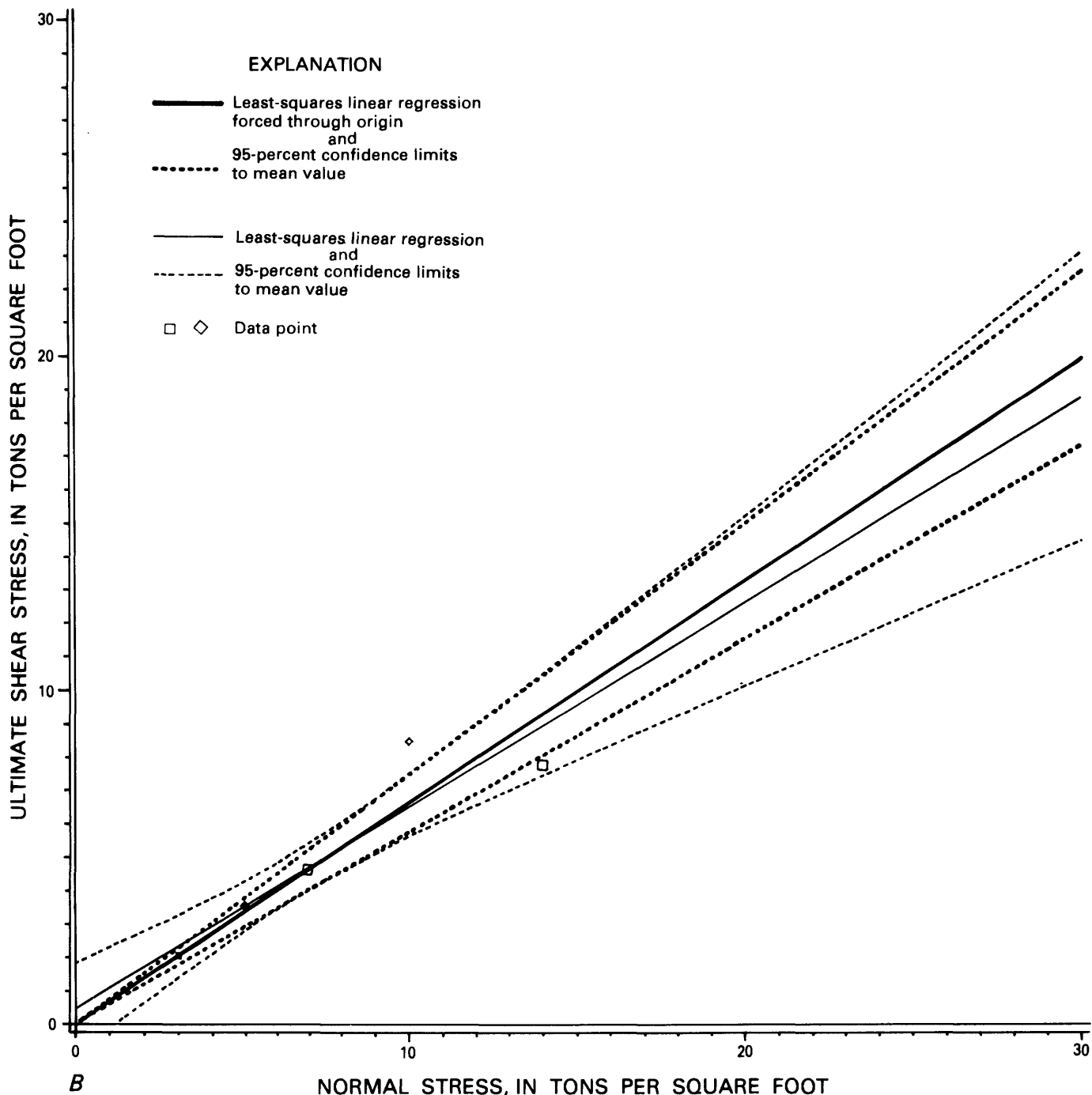


FIGURE 11.—Results of direct shear-strength tests on the ancestral dacite unit of the avalanche debris from various sites: *B*, ultimate strength.

ples from the ancestral dacite unit at other sites on the avalanche (table 2) are as follows: peak $\phi' = 31.6^\circ$ and $c' = 1.80$ tons/ft² ($r^2 = 0.775$); peak $\phi^* = 39.4^\circ$ ($r^2 = 0.942$), and ultimate $\phi^* = 33.5^\circ$ ($r^2 = 0.975$) (figs. 11A, B).

These results imply strength values somewhat lower than those given by Voight and others (1981) for samples distributed over the avalanche. They reported peak friction angles of about 38° to 44° for the same particle-size

range for nine avalanche samples. The analysis of the latter samples assumed zero cohesion, and thus their friction angles are comparable to values of ϕ^* determined during this study. Similarly, T. L. Youd and others (written commun., 1981) reported a peak angle of 42.5° for a single sample of debris-avalanche deposit. Both papers described reduction of friction angle (ultimate strength) as a function of displacement, and the validity of this concept is sustained by our results.

Several factors influence the cohesion values reported here. In some instances, sample heterogeneity has resulted in scattered data points on a Coulomb plot; linear regression results in a cohesion intercept that is more a reflection of data scatter than of finite strength at low normal pressure. In other instances, the data imply an intercept if a linear regression is assumed. Some workers might prefer to assume $c' = 0$ and to restrict strength envelopes to linear, or nonlinear, regression lines passing through the origin (Voight and others, 1981). The cohesions are generally considered "apparent" values, mainly reflecting incomplete saturation of test specimens during shear. Although breakage of angular grains might have occurred in some tests (particularly in some samples from the ancestral dacite unit of the debris-avalanche deposit), the reported cohesions do not represent reproducible strength components that can be relied on in analyzing slope stability.

GROUND-WATER CONDITIONS

In July 1983, the U.S. Geological Survey installed 11 piezometers in the South Fork Castle Creek blockage to determine ground-water levels. Water-level measurements taken on September 20, 1983 (after sufficient time had been allowed for the wells to recover from the effects of drilling and development), showed that a ground-water mound existed under the crest of the blockage (fig. 12). Water levels in the mound were as much as 22 ft above lake level at the time. Depth to water below the crest of the blockage in September 1983 ranged from about 60 to 20 ft, the greatest depth to water occurring in the northwestern part of the blockage and the least in the southeastern part. Water levels in the mound above lake level indicate that water moves from the mound into the lake and toward Castle Creek.

Ground-water levels in the blockage can be expected to fluctuate seasonally as the factors that affect ground-water recharge and discharge vary, but the lack of water-level measurements before July 1983 precludes definite determination of the amplitude of the changes. However, the timing of fluctuations should be similar to that observed in the similar blockage that created Coldwater Lake, 2 mi north of South Fork Castle Creek Lake on the opposite side of the North Fork Toutle River valley (fig. 1). Water levels in that blockage have been measured in

piezometers since July 1981 and have been observed to fluctuate seasonally, with annual highs in May and June and lows in September through October (fig. 13). The amplitude of these seasonal changes varies according to the location of the piezometer, but maximum changes of 15 ft have been observed along the crest of the blockage.

The 2-year record of ground-water levels at the Coldwater Creek blockage also showed a net annual increase in water levels—of 35 ft from August 1981 to August 1982 and 15 ft from August 1982 to August 1983. This indicates that discharge from the ground-water system in the Coldwater blockage has yet to equilibrate to natural recharge; this is an important consideration in analyzing the stability of the South Fork Castle Creek blockage. Because slope stability varies indirectly with ground-water levels, seasonal changes and the potential for annual increases in water levels in the South Fork Castle Creek blockage are important. Water levels shown in figure 12 can be assumed to be near their seasonal low and were used to formulate baseline conditions for the stability analyses that follow. Stability analyses for higher ground-water levels were also made and are discussed in the next section.

The proximity of the Coldwater Creek blockage to the South Fork Castle Creek blockage and the similarity of their composition suggest that water-level changes similar to those at the Coldwater blockage may be occurring at the South Fork Castle Creek blockage. Owing to differences in thickness, geometry, and other features of the blockages, the magnitude of the changes may be different, however.

STATIC SLOPE-STABILITY ANALYSIS

Factors of safety (F_s) were determined for five cross sections on the blockage by using a digital computer program, STABL3, prepared by the Joint Highway Research Project, Engineering Experiment Station, Purdue University. The program contains a subroutine that searches for slip surfaces most likely to fail. The program allows use of either the Modified Bishop Method or the Janbu Method of Slices for determining factors of safety associated with the model-predicted failure surfaces. The Modified Bishop Method was used throughout this study. As an independent check on the results, an analysis using the Morgenstern and Price Method was performed on a selected number of failure surfaces generated by STABL3; the resultant factors of safety were virtually identical (W. K. Smith, oral commun., 1982).

MODELED CROSS SECTIONS AND ASSUMPTIONS

Four of the five cross sections tested are on the downstream side of the blockage, in the area from the blockage crest toward Castle Creek (fig. 14). Of these four cross

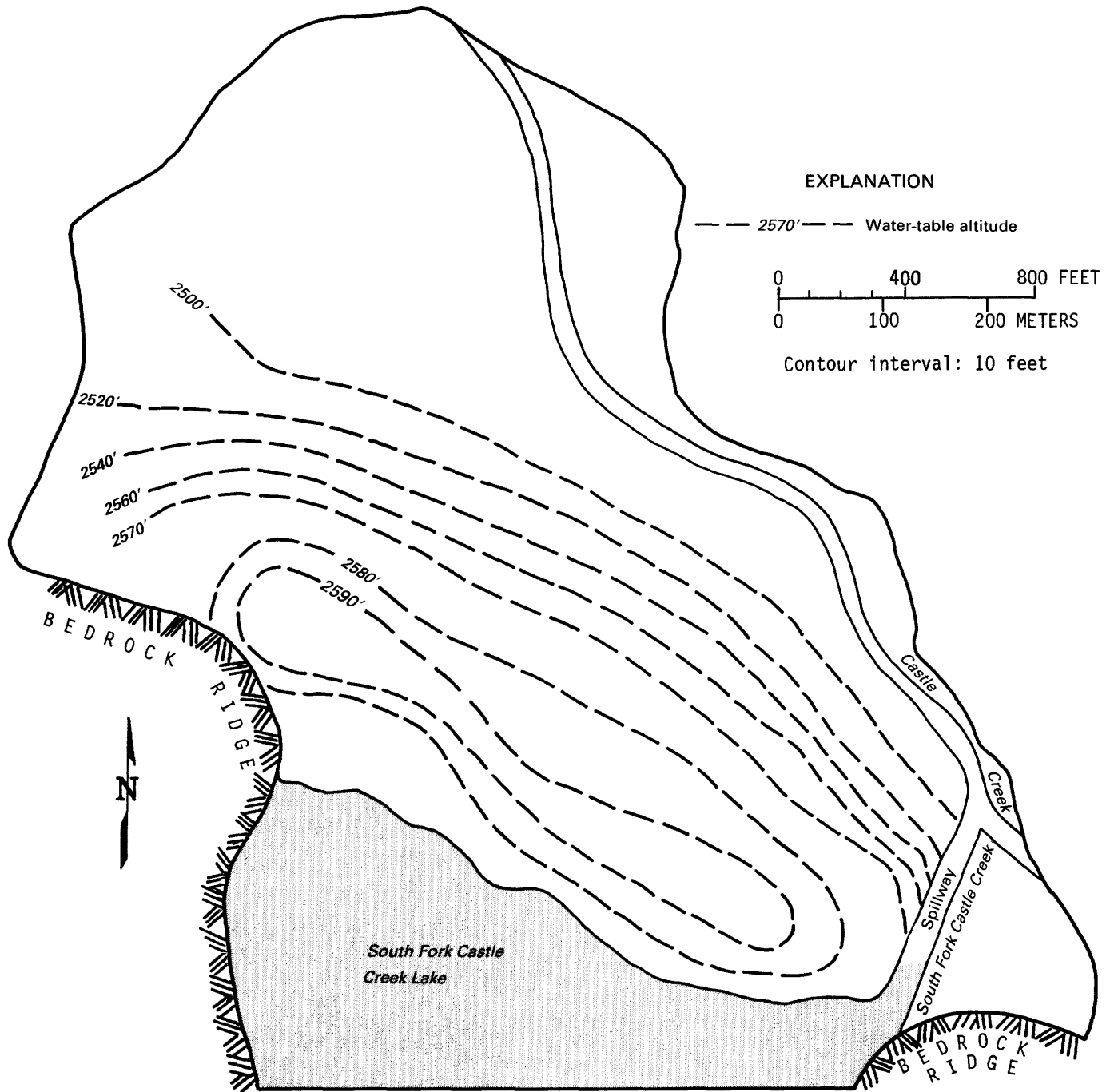


FIGURE 12.—Water-level contours for South Fork Castle Creek blockage, September 20, 1983.

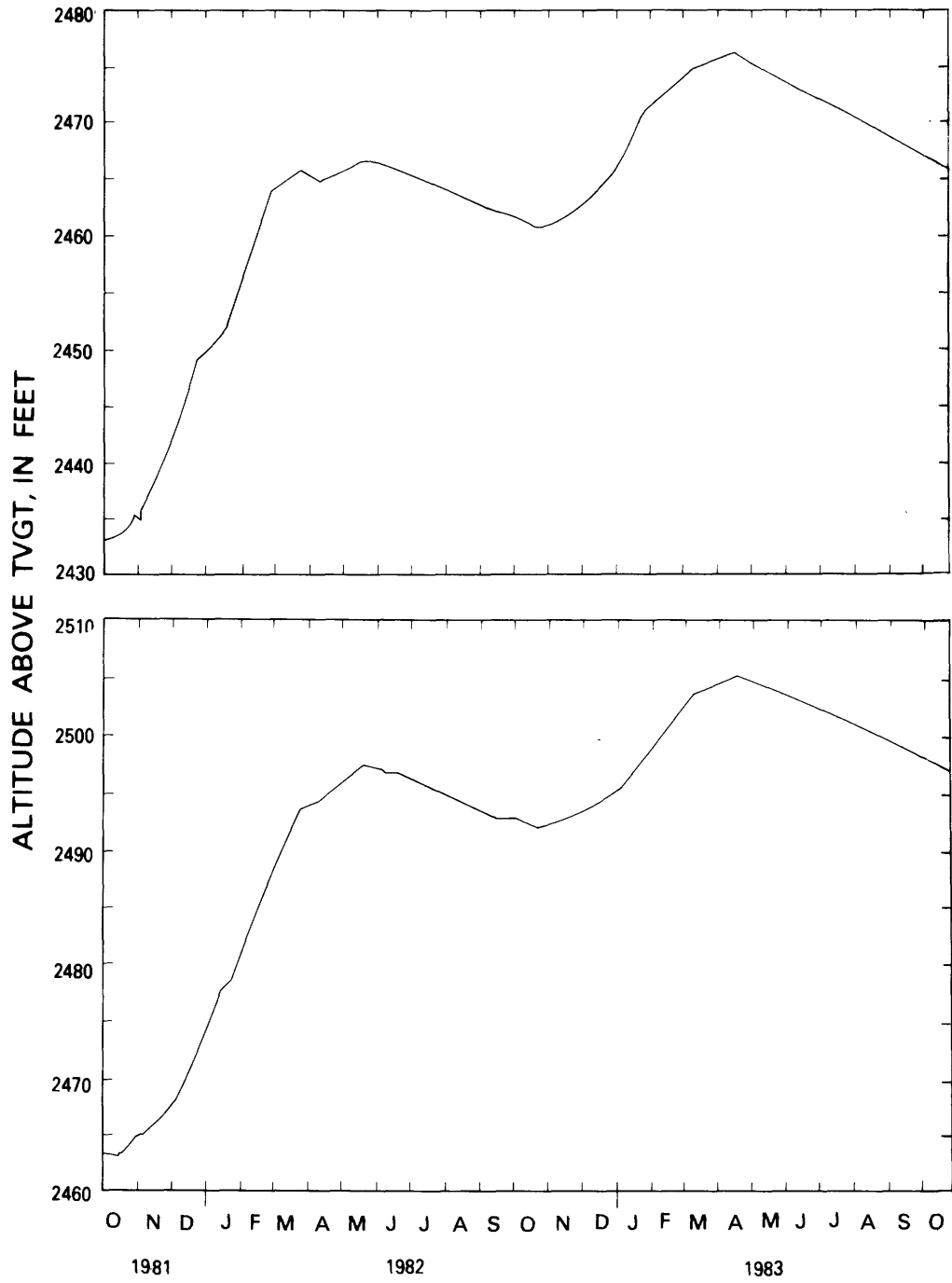


FIGURE 13.—Hydrographs for two selected piezometers at Coldwater Creek blockage.

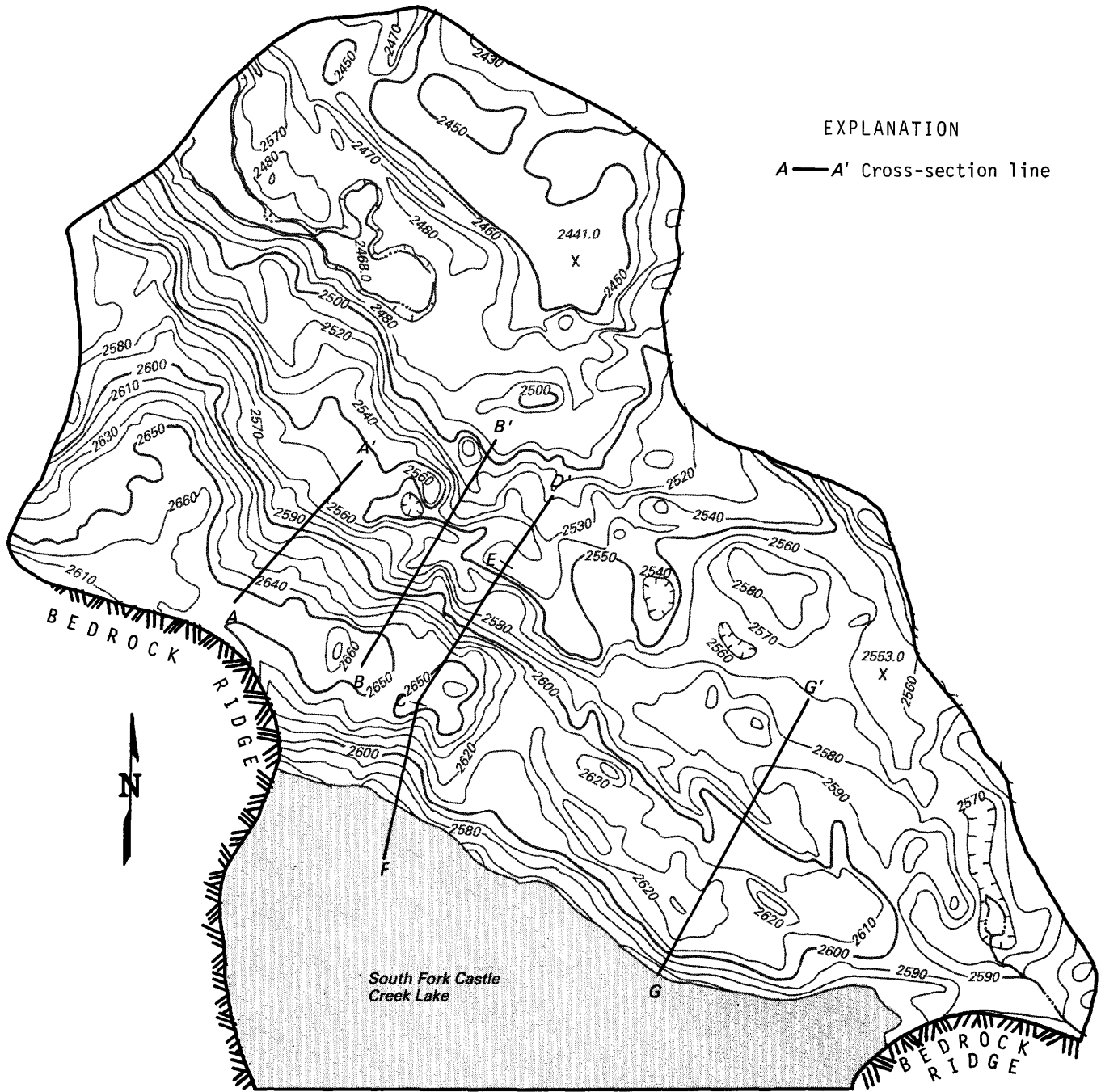


FIGURE 14.—Location of cross sections on South Fork Castle Creek blockage that were analyzed for slope stability.

sections, the three (AA', BB', and CD) on the western part of the blockage, where downstream surface relief is greatest, are representative of downstream areas most susceptible to slope failure. The fourth (GG') is representative of the eastern part of the blockage, where overall downstream relief is low. Surface geology, configuration of the preeruptive surface, and ground-water levels for September 8, 1983, were determined for these sections (figs. 15A-D). The modern dacite, andesite, and basalt unit is the predominant unit in all four cross sections.

Because slopes and subsurface conditions along the upstream side of the blockage, and the profile from the crest toward South Fork Castle Creek Lake, are generally uniform, one cross section, CF, was used to investigate the potential for slope failure in the upstream direction (fig. 15C).

At each cross section except GG', F_s was determined for six different conditions (four for GG'). In all cases, wet and saturated unit weights of 105 and 125 lb/ft³, respectively, were assumed. These estimates were made before the field and laboratory test programs were completed, and the assumed unit-weight values are now considered low. A sensitivity analysis was conducted to examine the influence of unit weights on predicted factors of safety. Extreme values for unit weights produced a change in F_s no greater than 0.1.

A friction angle of 35° was used for all analyses. This value is probably conservative because it approximates the laboratory ultimate for material from the modern dacite, andesite, and basalt unit rather than the peak (or some intermediate) condition, and the laboratory values ignore strength contributions from larger clasts and from moderate compaction. Because the ultimate friction angle for the blast pyroclastic-flow deposit and ancestral dacite unit is about 33.5°, the use of 35° may not be entirely conservative. Because the modern dacite, andesite, and basalt unit constitutes most of the blockage, 35° is considered reasonable for analytical purposes.

Using the above assumption, cohesion was set to zero and stability was determined at each cross section for three positions of the water table: (1) the measured water level for September 1983, (2) the September 1983 water level plus 25 ft, and (3) the water level at land surface. Cohesion was next set to 200 lb/ft² and stability was again determined for the three positions of the water table. At section GG', however, September 1983 water levels were about 20 ft below the crest, and therefore only water-level positions 1 and 3 were used—the September 1983 water level and the water level at land surface. These positions had values of cohesion at 0 and 200 lb/ft².

The program requires definition of a lower boundary that no generated failure surface will penetrate. The preeruption surface underlying the blockage was chosen as this boundary. Cross sections AA' and BB' are underlain by the bedrock ridge on the western side of South

Fork Castle Creek valley (figs. 15A, B), so the assumption of nonpenetration along those sections is valid. Cross sections DF' and GG' are underlain by prehistoric unconsolidated volcanoclastic deposits, however, and the assumption that this material represents a boundary that no generated failure surface could penetrate may not be valid. However, results of the computer analysis along these sections indicate that the surfaces most likely to fail are above the preeruption surface; potential failure along these sections is therefore independent of the nature of the preeruption surface.

Cross sections AA' and BB' terminate near the ridge bordering the western side of the lake. Slope failure along these sections would not result in a lake breakout unless this failure weakened the remaining blockage or unless it was accompanied by a failure back into the lake near these sections. The latter possibility does exist, and therefore stability in the areas of cross sections AA' and BB' is evaluated.

RESULTS OF STATIC SLOPE-STABILITY ANALYSIS

For each set of physical conditions used in a model simulation, the program generated 100 failure surfaces and calculated the factor of safety, F_s , for each surface. It also identified the surface with the lowest factor of safety, F_s^* , hereafter referred to as the critical failure surface. Model-predicted F_s^* values are summarized in table 3 for each set of physical conditions simulated at

TABLE 3—Model-predicted factors of safety (F_s^*) for critical failure surfaces at South Fork Castle Creek blockage for selected positions of the water table and cohesion values

[Stress friction angle, 0', equals 35°; factors of safety less than or equal to 1.2 are considered potentially unstable]

Position of the water table	Cross section	F_s^* for zero cohesion	F_s^* for 200 lb/ft ² cohesion
September 1983 - - - - -	AA'	2.1	2.4
	BB'	2.2	2.4
	CD	2.1	2.3
	CE	1.7	1.9
	CF	1.6	2.0
	GG'	4.1	4.3
September 1983 level plus 25 feet - - - - -	AA'	1.6	1.9
	BB'	1.8	2.0
	CD	1.4	1.9
	CE	1.2	1.4
	CF	1.2	1.5
At land surface - - - - -	AA'	0.8	1.1
	BB'	1.4	1.6
	CD	1.3	1.5
	CE	0.8	1.0
	CF	0.6	1.0
	GG'	2.4	2.8

the cross sections. A value of F_s less than or equal to 1.0 is considered to indicate potential instability. Although F_s values predicted by the model should be considered reasonable approximations of actual values, some uncertainties about material properties and analysis exist, and therefore factors of safety 1.2 or less are interpreted as identifying sections of potential instability.

Several general trends are apparent from the results of the static stability analysis. First, as ground-water levels rise, factors of safety for potential failure surfaces decrease, indicating that the blockage becomes less stable. This trend is illustrated in table 3. Second, rising ground-water levels also cause the range in values for the 10 lowest F_s surfaces to narrow (fig. 16), indicating that larger areas of the blockage become unstable. Third, for a given water level, analysis using a cohesion value of 200 lb/ft² shows an average increase in F_s^* of 0.3 over the F_s^* obtained with zero cohesion.

Results of the static analyses indicate that massive slope failures on the blockage due to gravitational forces are unlikely when the ground-water table is at or near its September 1983 position. F_s^* values for failure surfaces at all cross sections are above 1.2 for this condition. Potential failure is predicted on the blockage with ground-water levels 25 ft above September 1983 levels and zero cohesion. When the water table is assumed to be at land surface and zero cohesion is assumed, additional cross sections on the blockage are predicted to fail. These failures alone are not expected to initiate lake breakout because part of the blockage is left intact above lake level. Only cross sections BB' and GG' are stable for all three positions of the water table. The most conservative analyses for these sections, a water level at land surface and zero cohesion, are shown in figures 17A and B.

Prediction by the model of potential failure surfaces when the water table is assumed to be 25 ft higher than for September 1983 depends on the value used for cohesion. When a cohesion value of 200 lb/ft² is assumed, no slope failures are predicted. However, when zero cohesion is assumed, slope failures are predicted along cross sections CE and CF (table 3, fig. 18). The critical failure surface on cross section CE, with an F_s^* value of 1.2, extends 45 ft behind the crest of the blockage and 10 ft below lake level. On cross section CF, the critical failure surface has a value of $F_s^*=1.1$. Two other potentially unstable shallow failure surfaces occur where F_s values equal 1.1 and 1.2. Neither surface penetrates the blockage below lake level. Such failures occurring simultaneously along both cross sections would not result in lake breakout, because a substantial part of the blockage above lake level would be left intact.

With the water table at the land surface, potential failure surfaces predicted at cross sections AA', CE, and CF

when both zero and 200-pound-per-square-foot cohesion values are assumed. At cross section AA' the predicted failure surfaces are shallow and do not extend below lake level for either value of cohesion (figs. 19A, B). Therefore, these failures would have little influence on short-term blockage stability. At cross section CE, potential surfaces extend a maximum of 25 ft below lake level and 100 ft behind the blockage crest for zero cohesion (fig. 20A) and 50 ft behind the crest for 200 lb/ft² cohesion (fig. 20B). At cross section CF, potential failure surfaces are shallow and none extend below lake level when a 200-pound-per-square-foot cohesion value is assumed. However, assuming a cohesion value of zero, a potential failure surface of 1.2 extends about 30 ft below lake level and 50 ft behind the blockage crest. The critical failure surface does not extend below lake level and has an F_s^* value of 0.6. The potential failure surfaces along cross sections CE and CF that are predicted assuming both water level at land surface and zero cohesion, and that have F_s values <1.2, constitute a significant mass of the blockage, and some extend well below lake level. However, failure along both surfaces having F_s values of 1.2 (fig. 20A) would still leave a substantial part of the blockage intact and above lake level. Thus, lake breakout is not predicted for initial slope failures on the blockage, regardless of the position of the water table.

RETROGRESSIVE FAILURE ANALYSIS

Retrogressive slope failure was analyzed for composite cross section DF on the part of the blockage that remained after initial slope failures, assuming both water levels 25 ft higher than those in September 1983 and at land surface. The analysis included three assumptions considered to be conservative: (1) the material above the initial and all successive sliding surfaces is removed from the blockage, (2) retrogressive sliding occurs along the deeply penetrating surfaces having F_s values <1.2 and encompassing the greatest amount of blockage material, and (3) no slide mass will interfere with or influence the movement of successive slides. Zero cohesion was also assumed in all analyses.

Were the water table to rise 25 ft above its September 1983 position, retrogressive analysis indicates that the blockage would remain above lake level, thus precluding lake breakout (fig. 21). With the water table at land surface, analysis for retrogressive failure indicates that the blockage might be lowered below lake level, thereby causing lake breakout (fig. 22).

The degree of mobility necessary for breakout from retrogressive failure is considered unlikely, because the blockage is composed of moderately compact and poorly sorted debris, contains large clasts, and is subjected to moderate confining pressure. Slope failure would be more likely to occur in the form of debris slides,

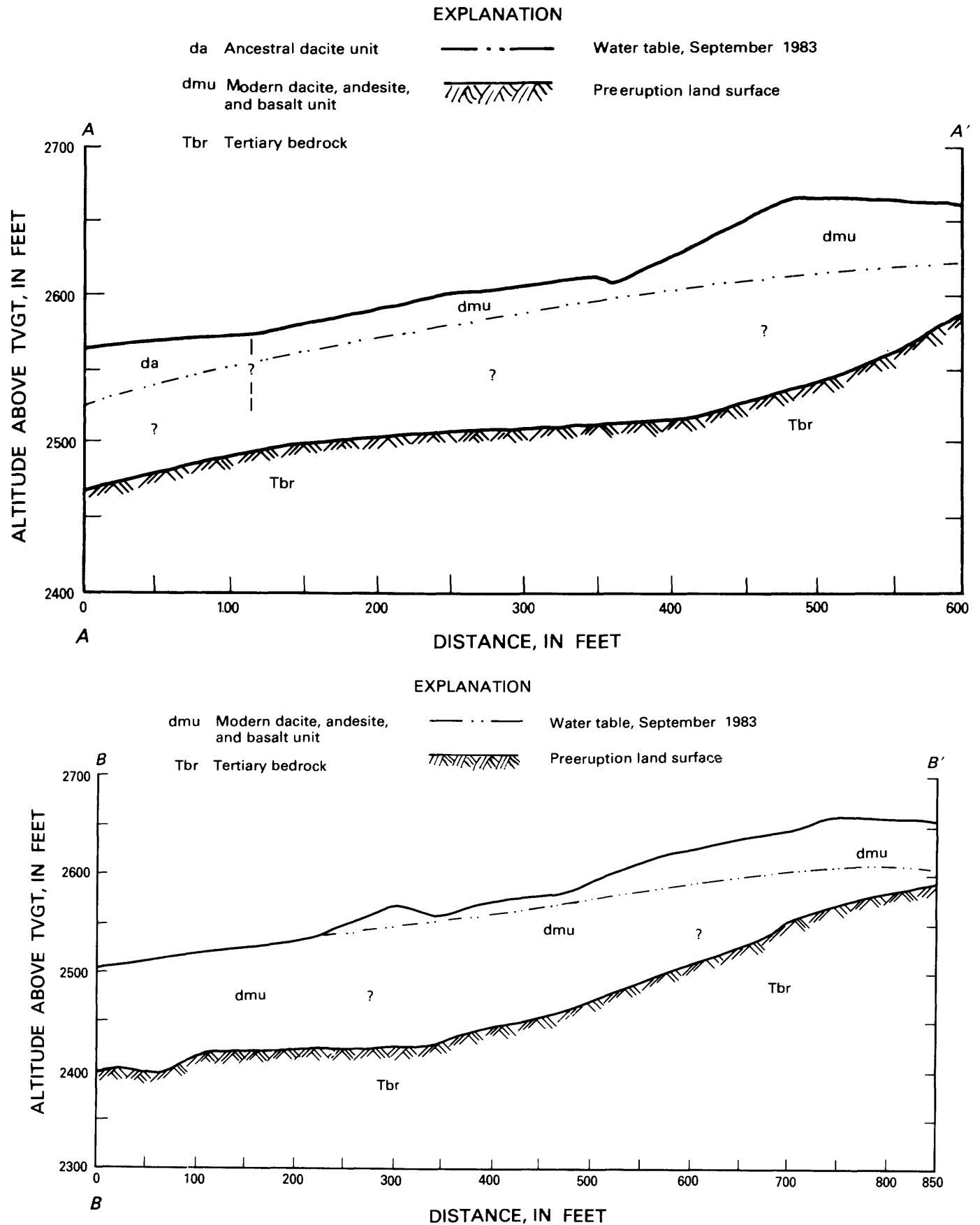


FIGURE 15.—Geology and September 1983 water levels at A, cross section AA' and B, cross section BB'.

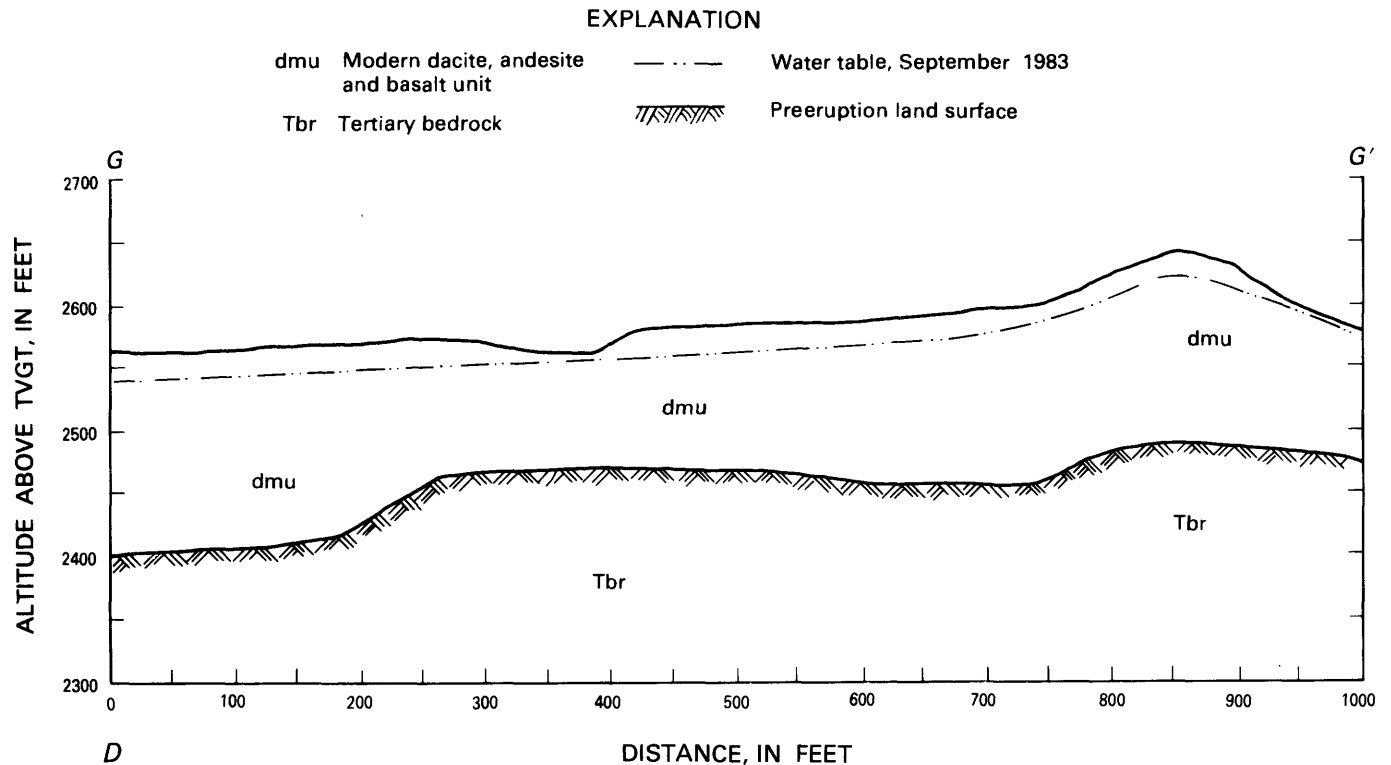
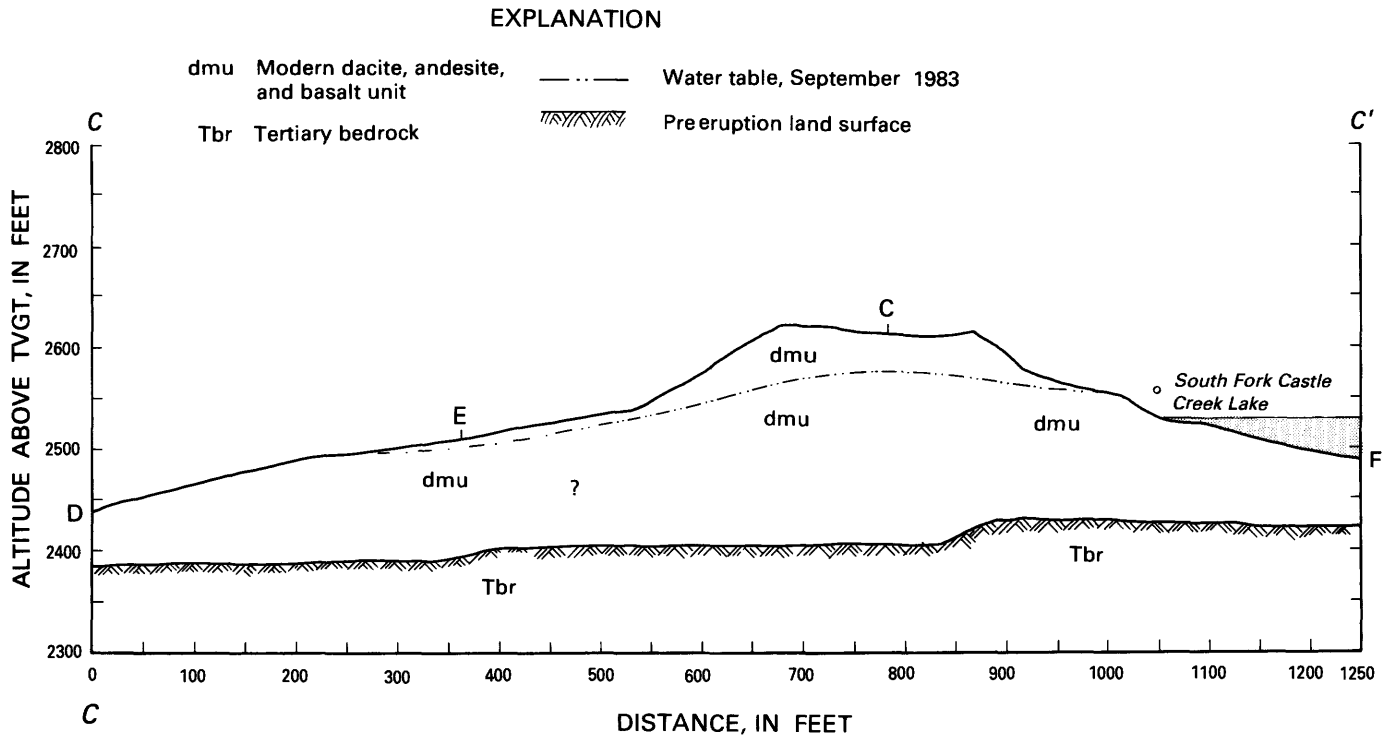


FIGURE 15.—Geology and September 1983 water levels at C, cross sections CD, CE, and CF and D, cross section GG'.

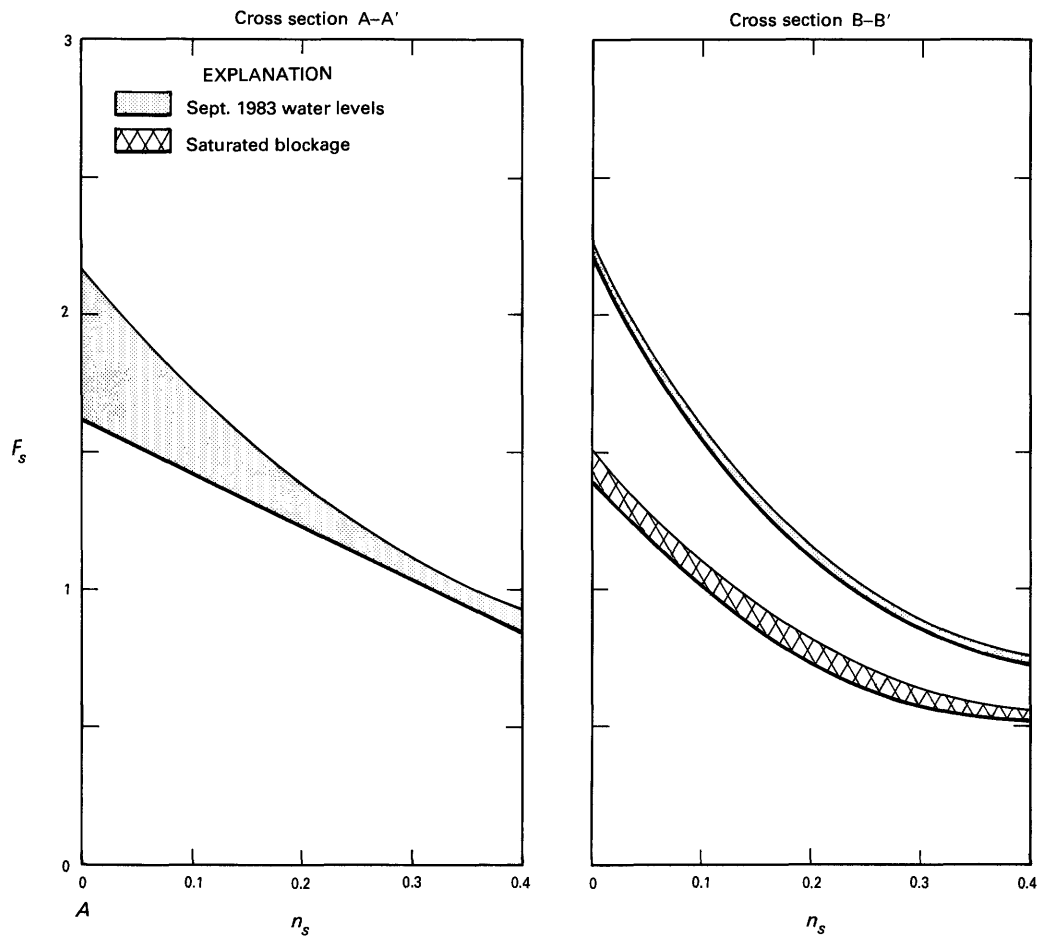


FIGURE 16A
Cross section C-D'

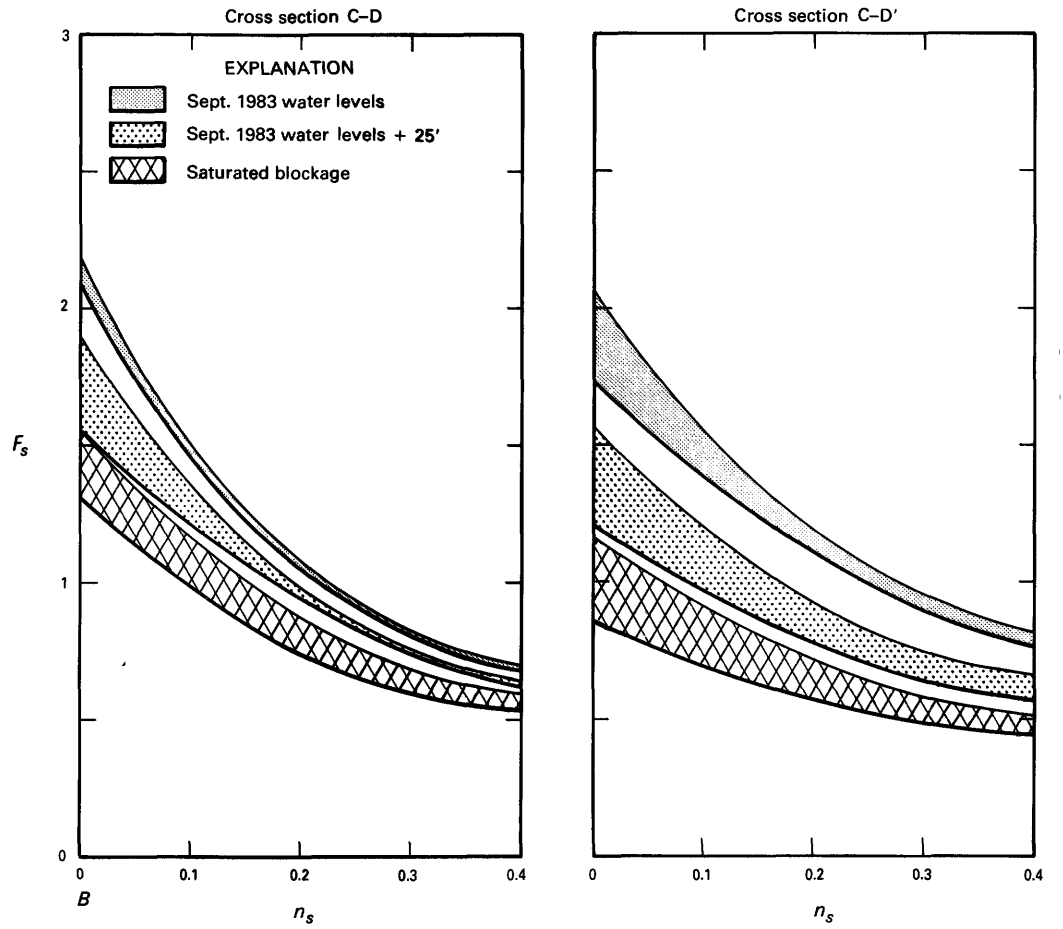


FIGURE 16B

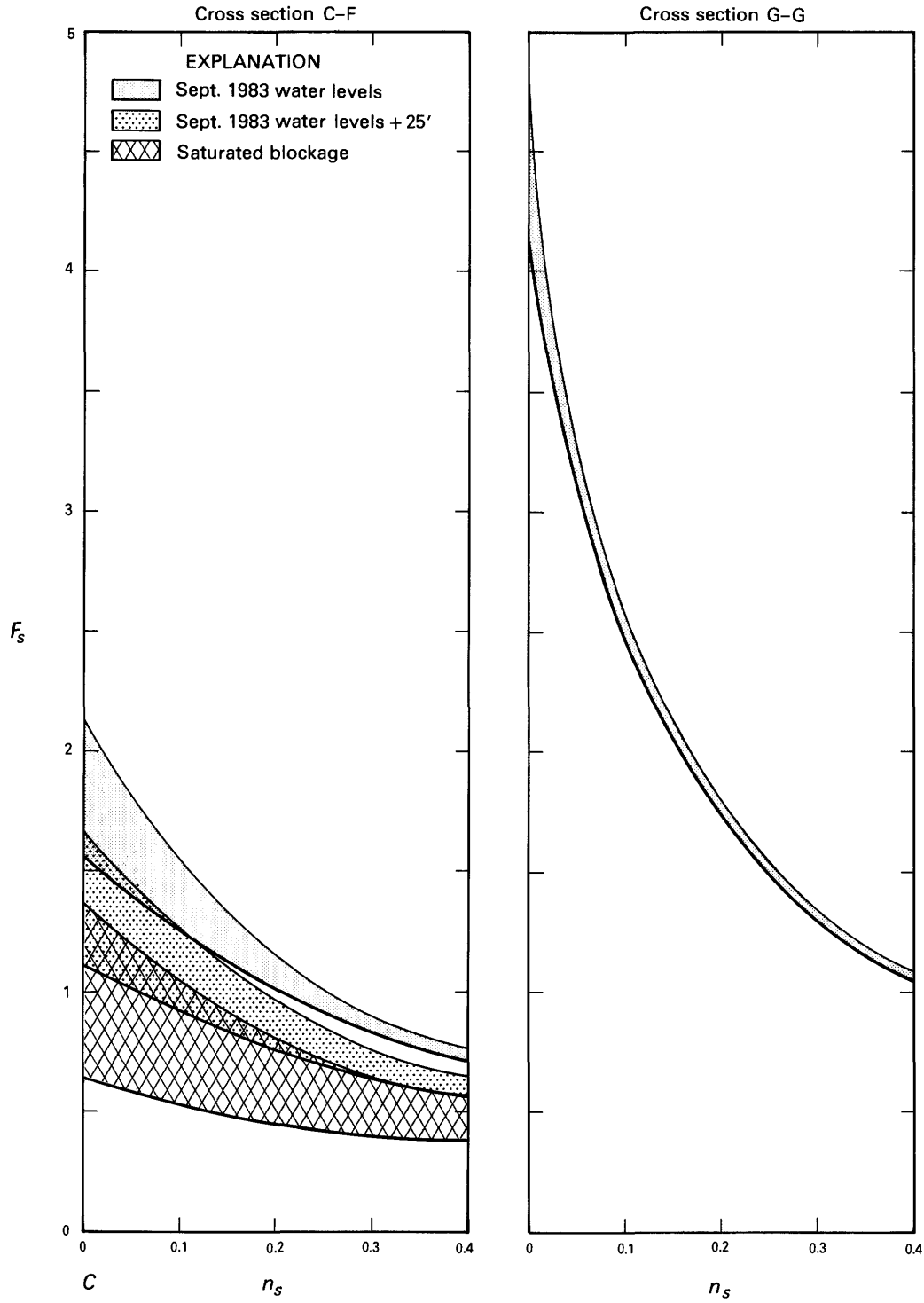


FIGURE 16C

FIGURE 16.—Variation of factor-of-safety values (F_s) versus seismic coefficients (n_s) for selected water levels at all cross sections.

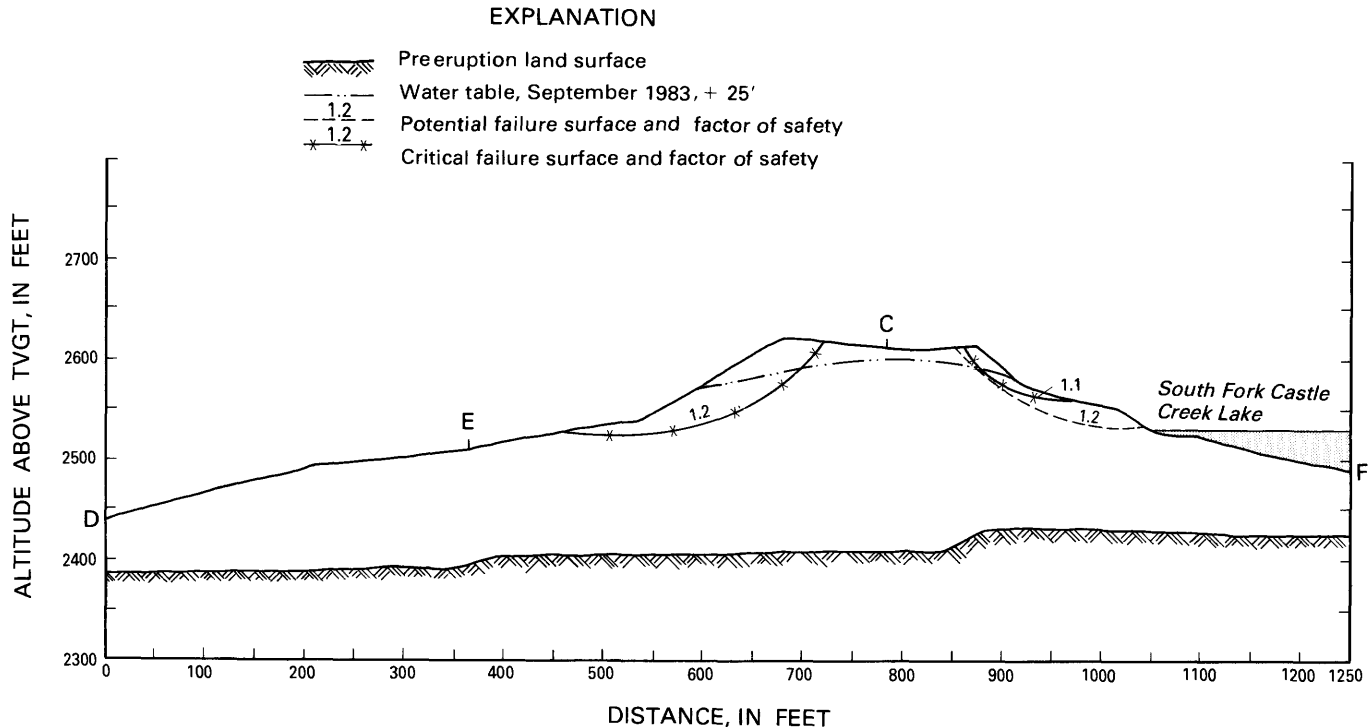


FIGURE 18.—Critical failure surface and potential failure surface encompassing the largest section of the blockage for cross sections *CE* and *CF* with water table 25 ft above September 1983 levels and zero cohesion.

slumps, and slump flows, and flowage at the toe of the displaced mass would be slow. Driving forces decrease and resisting forces increase as a function of displacement on deep-seated, curved slide surfaces, so displacements would be limited and would seldom exceed a value of approximately 100 ft. Movements of this order of magnitude would not be sufficient to lower the blockage crest to lake level or below. Therefore, the possibility of actual lake breakout from retrogressive slope failure is considered remote.

SEISMIC HAZARD

Estimates of the seismic hazard at the South Fork Castle Creek blockage are based primarily on information about the St. Helens seismic zone (SHZ), which passes within several miles of the blockage (fig. 1). Defined by earthquakes of small to moderate magnitude (2.5–5.5 local Richter magnitude), the SHZ is interpreted as a 60-mile-long fault zone capable of generating a shallow (crustal) earthquake of moderate to large magnitude (Weaver and Smith, 1983). Earthquake focal mechanisms along the SHZ indicate nearly vertical right-lateral, strike-slip faulting with the preferred fault planes striking north–south. From these focal mechanisms, the direction of maximum compression would appear to be northeast, approximately parallel with the direction of convergence between the North

American and Juan de Fuca plates. The focal mechanism data suggest “locked” subduction, and this interpretation raises the possibility of a subduction earthquake of larger magnitude (Weaver and Smith, 1983).

An earthquake of magnitude 5.5 (local Richter magnitude) occurred on February 14, 1981, near Elk Lake, 6.5 mi north of the South Fork Castle Creek blockage (Grant and others, 1984). More than a thousand aftershocks up to magnitude 4.5 delineated a north–south-trending fault zone 4 mi long by 2 mi wide, ranging from 3 to 8 mi in depth. The probable low-stress drop of the main shock suggests that preexisting stress levels were not extensively lowered and that another moderate earthquake may still occur near Elk Lake (Grant and others, 1984).

The occurrence of an earthquake larger than 5.5 magnitude along the SHZ must also be considered a possibility. Using empirical regressions of magnitude with fault length (Mark and Bonilla, 1977), a magnitude 7 earthquake would correspond approximately with a rupture of 50 percent of the length of the SHZ. However, Weaver and Smith (1983) recognized that there is no reliable procedure for estimating a maximum magnitude for the 1983 circumstances, and they considered a magnitude 7 earthquake unlikely for two reasons. First, Mount St. Helens is in the middle of the zone and the zone may be discontinuous across the mountain.

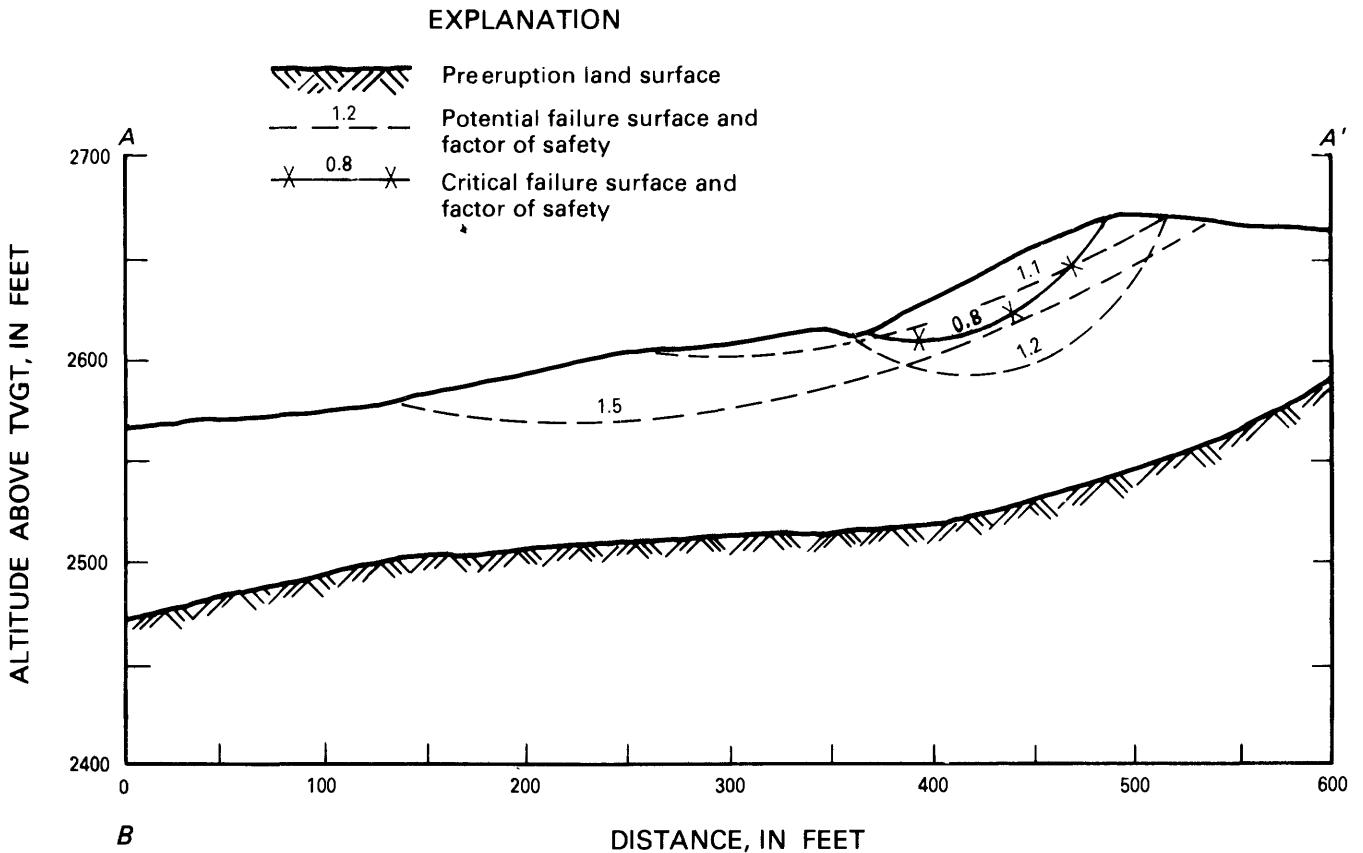
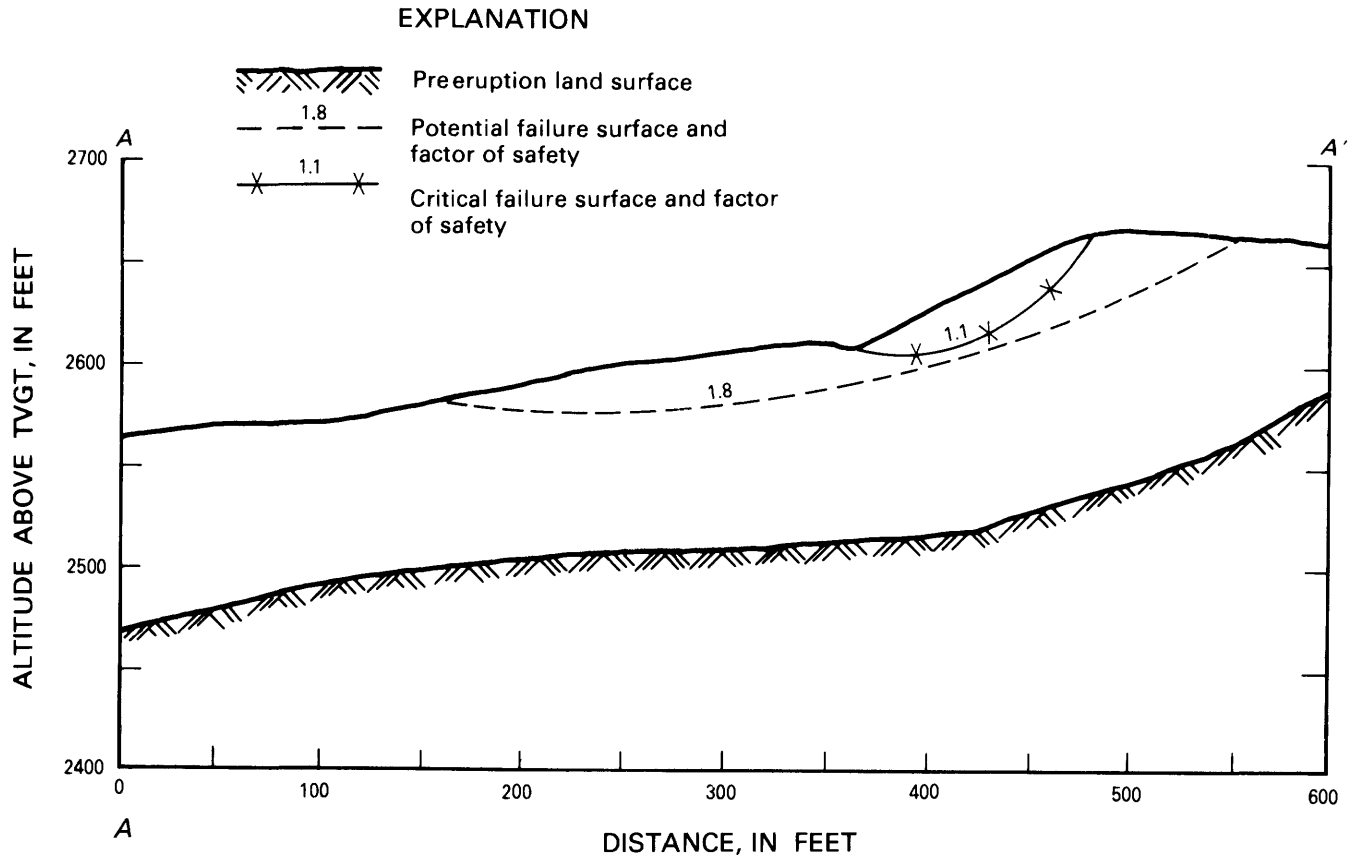


FIGURE 19.—Critical failure surfaces predicted for cross section AA' with water table at land surface and A, 200 lb/ft² cohesion and B, zero cohesion.

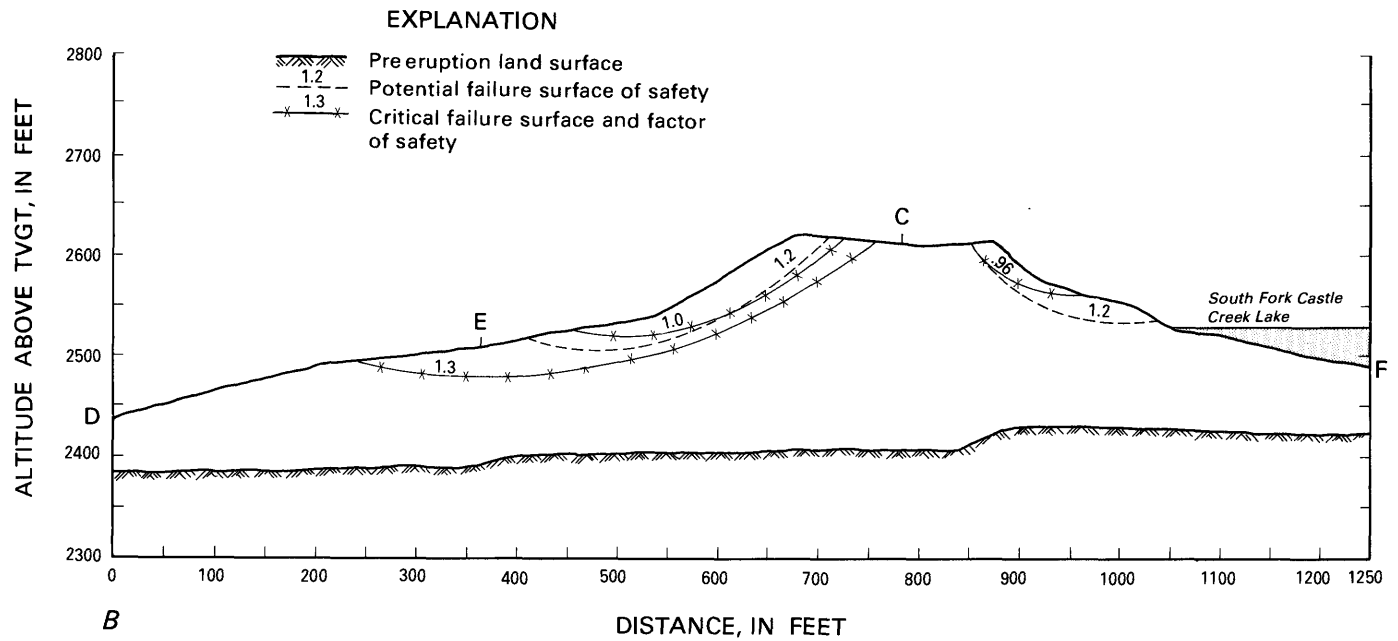
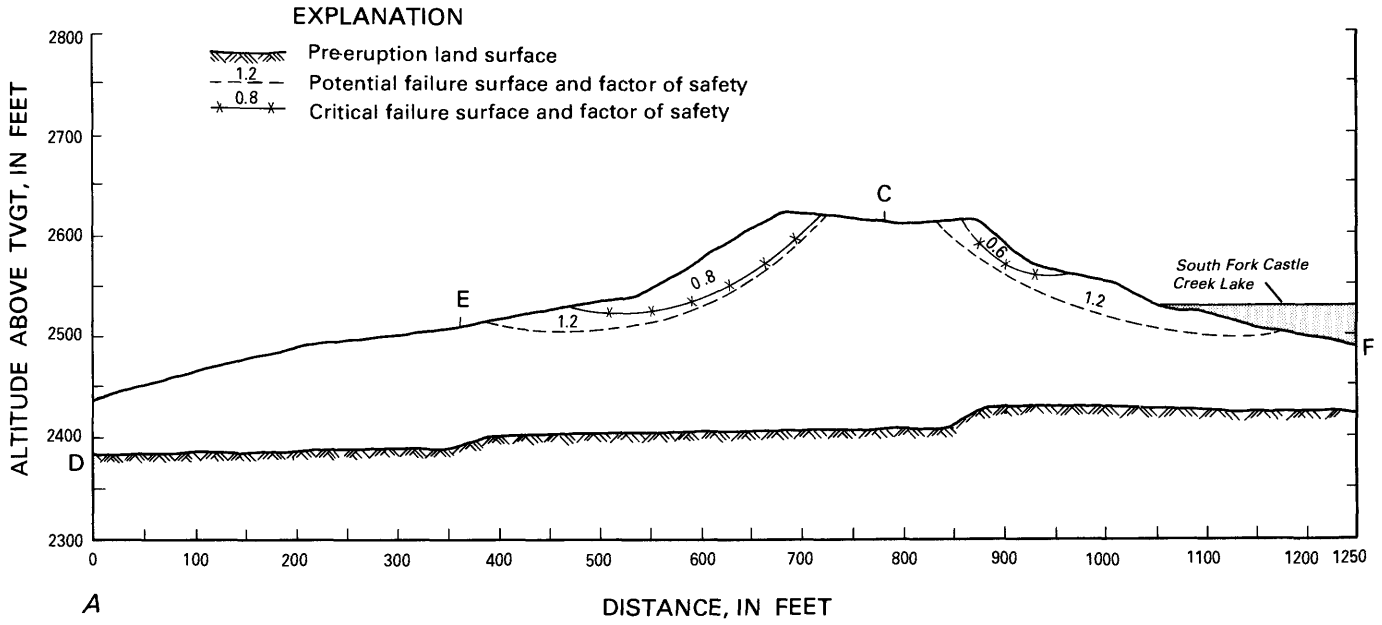
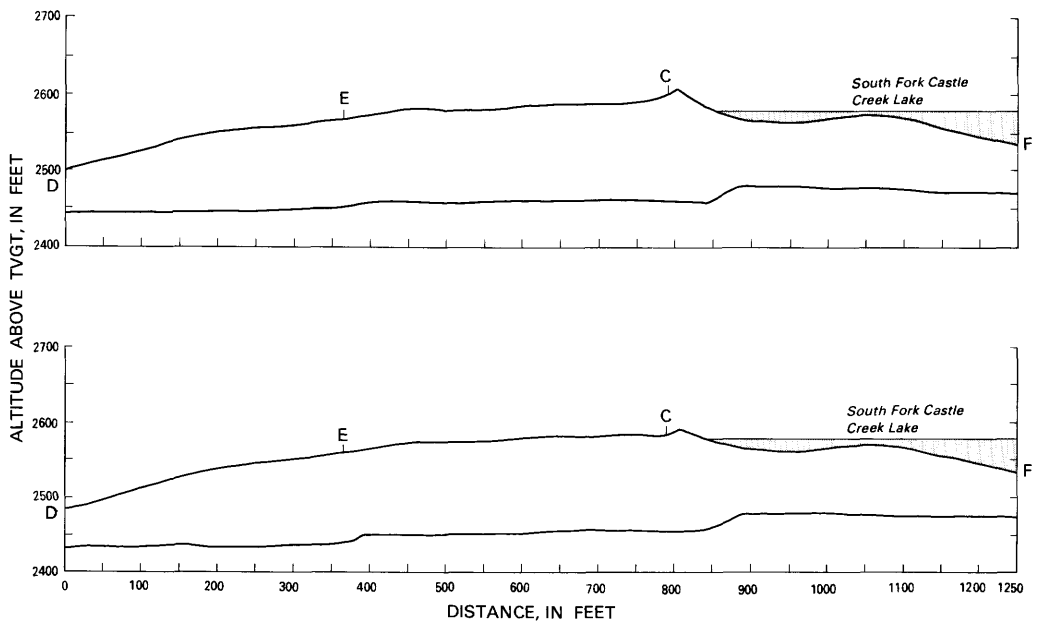
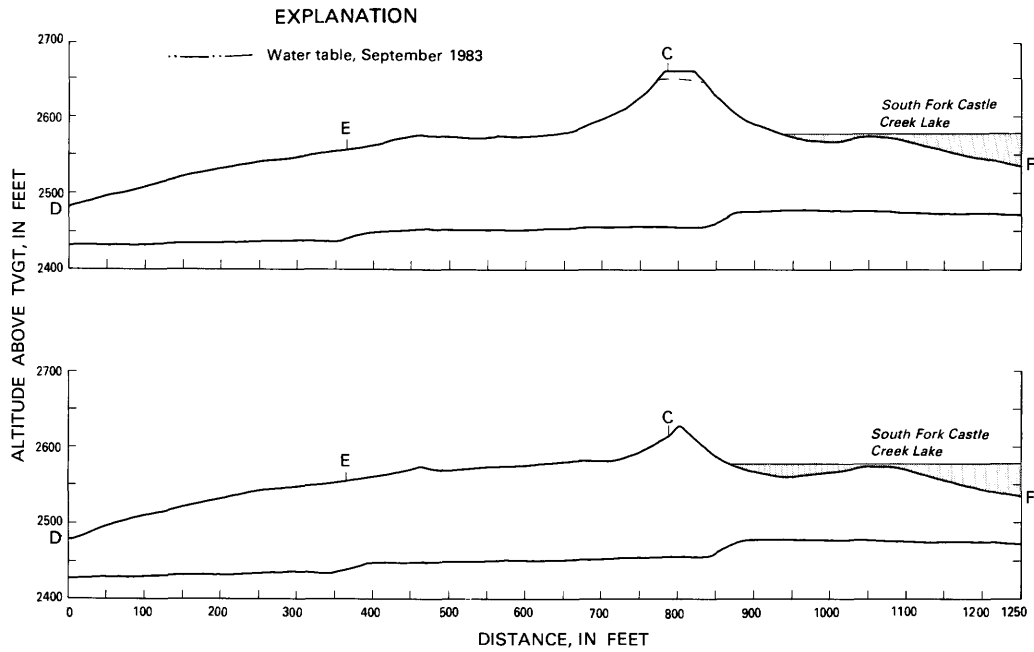
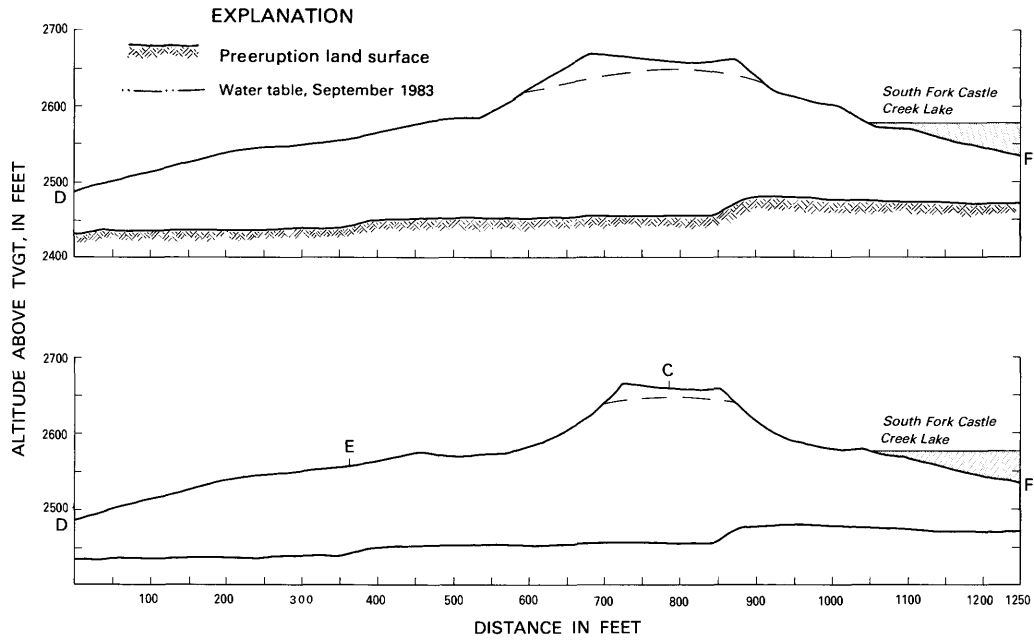


FIGURE 20.—Critical failure surface and potential failure surface encompassing the largest section of the blockage for cross sections *CE* and *CF* with water table at land surface and *A*, zero cohesion and *B*, 200 lb/ft² cohesion.



Second, the earthquakes are in a zone several miles wide in which no surface faulting has been found; therefore, the crustal earthquakes could involve rupture of short fault segments, on the order of, say, 6 mi. Weaver and Smith did not specify an expected maximum magnitude but did caution that the Elk Lake earthquake does not represent the largest possible event on the SHZ. Beaulieu and Peterson (1981), in an evaluation of potential hazards at a nearby nuclear site, suggested that a maximum magnitude of 6.2 is more likely than one of 7.

The U.S. Army Corps of Engineers proposed a magnitude 6.8 design earthquake for their stability analysis of the Spirit Lake blockage (U.S. Army Corps of Engineers briefing, July 5, 1983, Portland, Oreg.). This design earthquake would lie on the SHZ and have a near-source horizontal acceleration of 0.55 g, a shaking velocity of 1.8 ft/s, and a duration of strong shaking of 30 s.

Earthquakes along the SHZ in the magnitude range of 6.2–6.8 are capable of producing peak horizontal accelerations of 0.55 g at the South Fork Castle Creek blockage (H. B. Seed, written commun., 1983), so this acceleration value seems reasonably conservative for seismic analysis of the blockage. For purposes of comparison, a magnitude 5 earthquake on the Spirit Lake segment of the SHZ could produce peak accelerations of 0.3 g for two or three loading cycles at the blockage.

SEISMIC HISTORY OF THE BLOCKAGE

Since its emplacement on May 18, 1980, the South Fork Castle Creek blockage has been subjected to three periods of shaking. The first occurred during the 10 minutes of emplacement of the debris avalanche when the levee constituting the blockage was deposited before the remainder of the avalanche had come to rest. Ground vibrations associated with avalanche emplacement were considerable (Stephen Malone, oral commun., 1983); it is conceivable that the blockage was subjected to accelerations on the order of 0.1 g for several minutes. The second occurred from 11:40 a. m. to 5:30 p. m. (Pacific daylight time) on the same day, when numerous shocks associated with the Plinian eruption of Mount St. Helens produced strong shaking. The blockage was subjected to peak accelerations on the order of 0.05 to 0.1 g (Stephen Malone, oral commun., 1983). Finally, the Elk Lake earthquake of February 14, 1981, could have produced peak accelerations of 0.2 g at the blockage for several cycles.

FIGURE 21.—Predicted results of retrogressive slope-failure analysis on cross sections CD and CF with September 1983 water levels plus 25 ft and zero cohesion.

The effects of these events on the debris-avalanche deposit have not been studied, but it is presumed that the ground vibrations produced compaction of the deposit and increased its relative density. Ground-water levels in the blockage at the time of these shaking events were probably lower than those measured in September 1983.

DYNAMIC SLOPE-STABILITY ANALYSIS

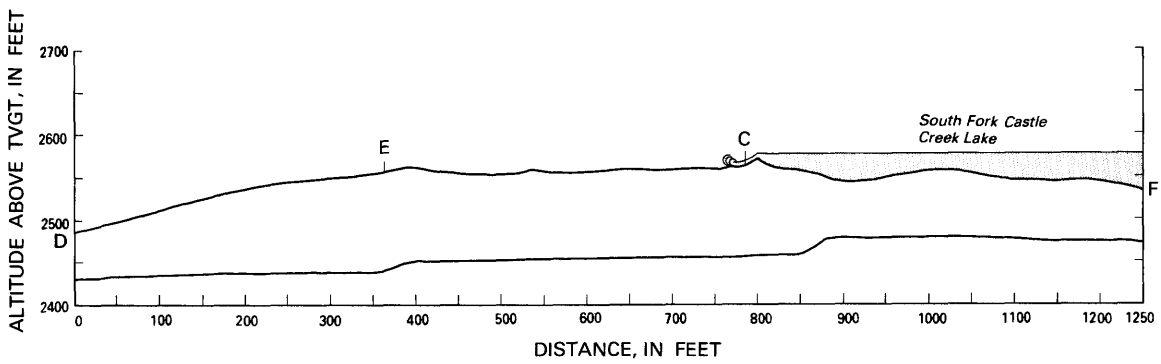
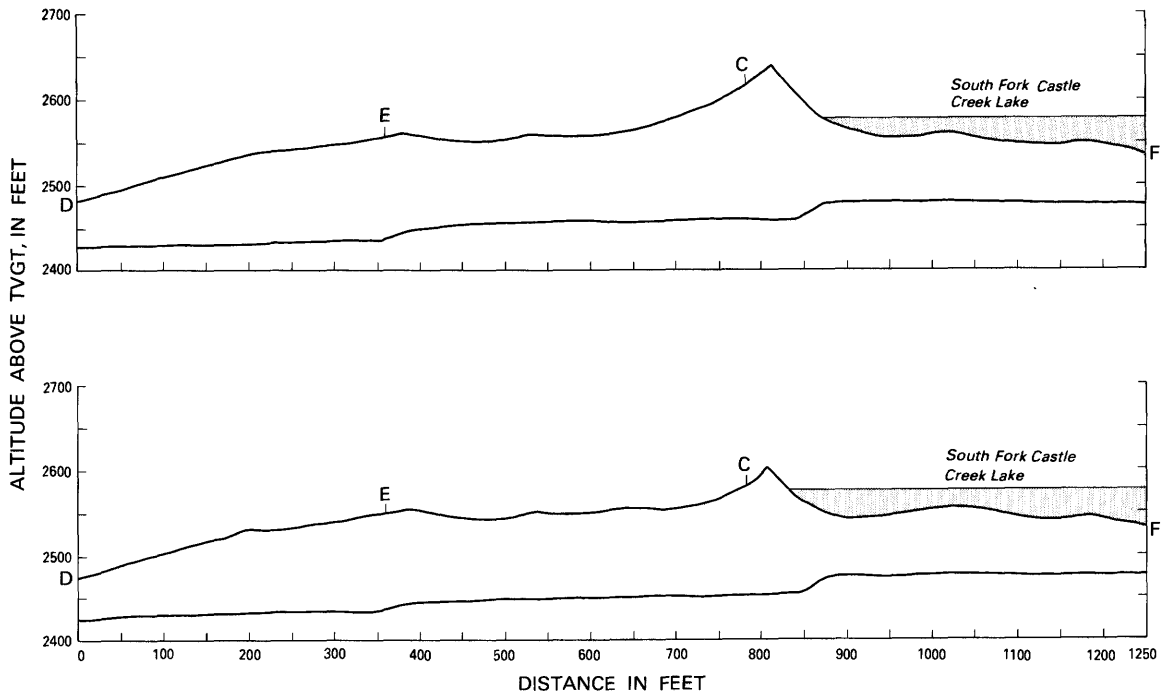
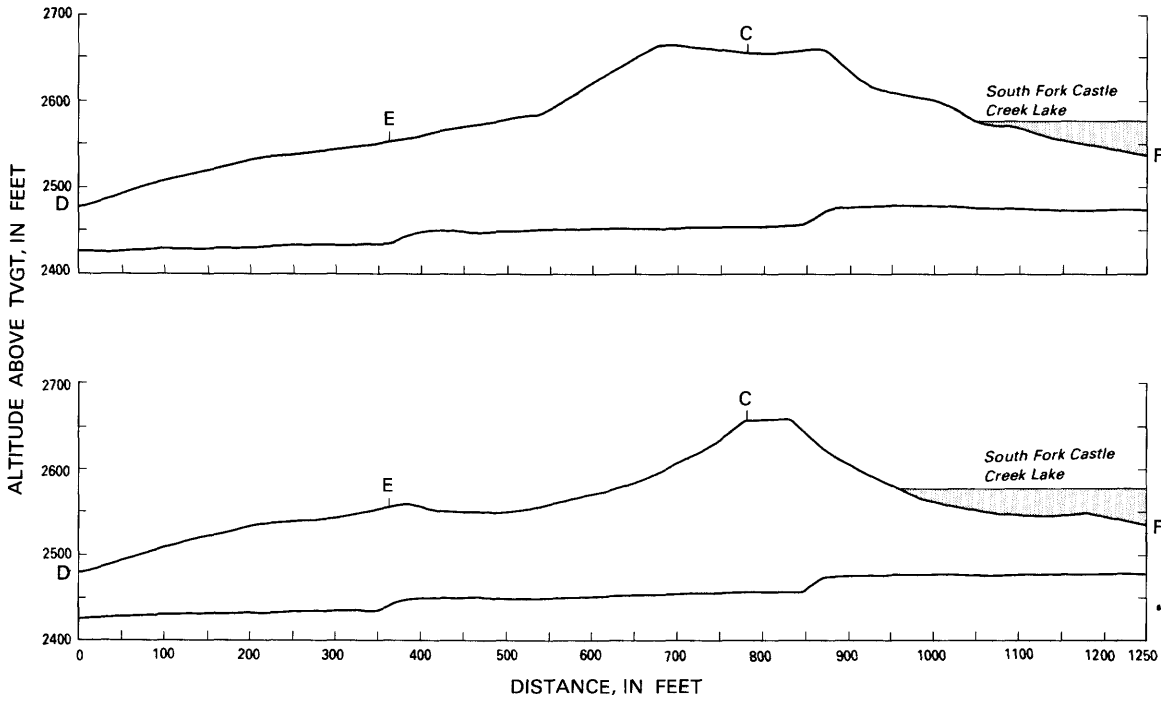
STABL3 contains an optional program that allows determination of the approximate effect of an earthquake the factor of safety; this program was used to determine F_s values, for two levels of earthquakes, at all the cross sections previously tested for static stability. In using this program, the assumption is made that dynamic loading from an earthquake can be replaced by a static horizontal force that is obtained from the product of the weight of the potential sliding mass and a seismic coefficient, n_s . Under this assumption, the section may be considered unstable if F_s approaches 1.0, but there is no theoretical basis to support this. Among other things, the value of n_s varies directly with earthquake magnitude, and two values of n_s were used in the analysis, 0.2 g and 0.4 g. As will be discussed subsequently, the larger value is believed to correspond closely to the seismic coefficient of the maximum credible earthquake for the SHZ. The maximum credible earthquake is believed to be near, but greater than, magnitude 6.0.

MODELED CROSS SECTIONS AND ASSUMPTIONS

F_s values for all cross sections were determined for seismic coefficients equal to 0.2 and 0.4 g and for water levels at their September 1983 positions. In addition, F_s values for cross section CD, CF, CE, and BB were determined for the range in seismic coefficients indicated above and for ground-water levels 25 ft above their September 1983 configuration, as well as for water levels at land surface. Wet and saturated unit weights of 105 and 125 lb/ft³, respectively, were assumed in all analyses. For all analyses, zero cohesion and a drained friction angle of 35° were used with the additional assumptions previously discussed under "Static Slope-Stability Analysis."

CALCULATION OF n_s

Methods of assigning seismic coefficient values include selecting an empirical value, assuming rigid-body response, or using viscoelastic-response analysis. Because the last method provides a more rational approach, it was used to estimate a value for n_s that could be assigned to the blockage for the maximum credible



earthquake along the SHZ. The value was obtained from the relationship:

$$\bar{n}_s(t) = \frac{1}{W} \sum_{\lambda} m(y) \ddot{u}_a(y), \quad (1)$$

where W is weight of sliding mass, m is an incremental horizontal slice of the mass, and \ddot{u}_a is the absolute acceleration at each instant, t , under consideration; y is the vertical coordinate direction (Seed and Martin, 1966). It is necessary to specify boundaries of the sliding mass in order to compute average seismic coefficients, leading to a different average n_s value for each potential mass at any instant of time. The matter is simplified by representing each sliding mass as a triangular wedge, thus permitting the average seismic coefficient over a given depth to be computed directly. For given values of embankment shear-wave velocity, damping factor, and embankment height, values of $\bar{n}_s(t)$ can be computed for any particular ground-motion record.

For the September 1983 case, the blockage is assumed to be homogeneous, with a shear-wave velocity of 1,000 ft/s and 20 percent critical damping. The north-south component of the 1940 El Centro earthquake, with duration of 0 s, is assumed for analysis, with the peak acceleration scaled to 0.55 g. Calculations presented by Seed and Martin (1966) then allow direct estimation of seismic parameters. Seismic coefficients thus determined vary considerably as a function of time (Seed and Martin, 1966, with ordinate values multiplied by 1.70). For September 1983 purposes, the variation in seismic coefficients is approximated by an equivalent number of acceleration cycles of constant amplitude. The fundamental period of the blockage foundation system is about 0.5 s at cross section DF. An equivalent seismic force series might be approximated by 10 cycles of force with a predominant frequency of 1.8 cycles/s, yielding, to one significant figure, the following amplitudes of average seismic coefficient $\bar{n}_s(t)$: 0.6 g (for potential slide masses in the upper quarter of blockage), 0.5 g (for the upper half), and 0.4 g (for the upper three-quarters or full blockage height).

Thus, average seismic coefficients vary considerably with position in the blockage material, as well as with time, and higher values occur with increasing altitude. This latter consideration is significant, because it influences the position of the most critical failure surface.

RESULTS OF DYNAMIC SLOPE-STABILITY ANALYSIS

General results of all the dynamic analyses indicate that for a given position of the water table increasing earthquake magnitudes cause F_s and F_s^* values to decrease and potential failure surfaces to occur deeper in the blockage than they do in the results of the static analysis. All cross sections on the blockage, including those that were stable for all positions of the water table under static analysis, become unstable during shaking induced by earthquakes near the maximum credible value, even for September 1983 water levels. In addition, for an earthquake of given magnitude, rising ground-water levels cause F_s and F_s^* values to decrease, and in some cases they cause potential failure surfaces to penetrate deeper into the blockage. Decrease in values of F_s and F_s^* as a result of increasing earthquake magnitude and ground-water levels is shown in figure 16. Each zone shown in the figure represents a given water-level condition and is bounded by the maximum and minimum F_s values for the 10 surfaces predicted by the model for each analysis. In addition to decreasing, the range in values for the 10 low F_s surfaces also narrows considerably.

Reduction in F_s and F_s^* values caused by increasing earthquake magnitudes and by increasing ground-water levels is significant. Table 4 shows this reduction for both conditions, and, as can be seen, values of F_s^* fall below unity along many sections for higher n_s values and (or) higher ground-water levels. F_s^* values are below unity for all sections except GG' for $n_s=0.49$ g, regardless of the position of the water table. They are also below unity for water levels 25 ft higher than in September 1983 and $n_s=0.2$ g on all cross sections tested for this set of conditions. Narrowing of the range of the 10 low F_s surfaces shown in figure 16, combined with the reductions in F_s and F_s^* , indicates that larger areas of the blockage become potentially unstable as earthquake magnitudes and ground-water levels increase.

Deformation over the entire blockage would be possible if an earthquake of a magnitude near 6.0 occurred when water levels were at their September 1983 position. Critical failure surfaces at all cross sections except AA' extend below lake level; the deepest extends approximately 120 ft below lake level and 100 ft behind the crest of the blockage. The model does not predict that any of these initial failures would result in immediate lake breakout, because, even if slippage occurred simultaneously from the crest toward the lake and from the crest toward Castle Creek, a part of the blockage would remain intact and above lake level.

If a smaller earthquake ($n_s=0.2$ g) occurred with water levels at their September 1983 position, considerable de-

FIGURE 22.—Predicted results of retrogressive slope-failure analysis on cross sections CD and CF with water table at land surface and zero cohesion.

TABLE 4.—Model-predicted factors of safety (F_s) for selected seismic coefficients (n_s)

Cross section	Water-table position	$n_s = 0$	$n_s = 0.2$	$n_s = 0.4$	Remarks on critical surfaces
AA' - - - - -	Sept. 1983 level - - - - -	*2.10	*1.20	*0.90	Shallowest surface of 10 predicted.
BB' - - - - -	Sept. 1983 level - - - - -	*1.40	*1.10	*.70	Shallow $F_s = 1.4$ surface, figure 17A.
	At land surface - - - - -	1.41	*.76	*.52	
CD - - - - -	Sept. 1983 level - - - - -	*2.10	*1.11	*.69	Shallow surface passing below slope break.
	Sept. 1983 level plus 25 ft - - - - -	*1.64	.92	.63	
	At land surface - - - - -	*1.30	*.76	.53	
CE - - - - -	Sept. 1983 level - - - - -	*1.70	*1.11	*.76	$F_s = 1.2$ surface, fig. 18.
	Sept. 1983 level plus 25 ft - - - - -	*1.20	*.78	*.57	
		1.46	.83	.58	$F_s = 0.8$ surface, fig. 20. Shallower than $F_s = 0.8$ surface, fig. 20.
	At land surface - - - - -	*.82	*.57	.44	
	.86	.57	*.43		
CF - - - - -	Sept. 1983 level - - - - -	*1.60	*1.05	*0.72	$F_s = 1.1$ surface, fig. 18.
	Sept. 1983 level plus 25 ft - - - - -	*1.11	*.76	.56	
		1.24	.78	*.56	$F_s = 1.2$ surface, fig. 18. $F_s = 0.6$ surface, fig. 20. $F_s = 1.2$ surface, fig. 20.
	At land surface - - - - -	*.63	*.47	*.38	
	1.18	.70	.50		
GG' - - - - -	Sept. 1983 level - - - - -	*4.10	*1.71	*1.05	

*Critical value of factor of safety.

formation of the blockage also would be possible. The model predicts potential failure surfaces at all sections except GG', where F_s^* is 1.7. The greatest potential instability occurs along cross section DF, where potential failure surfaces reach their maximum distance below lake level (fig. 23). Once again, however, the model does not predict immediate breakout, because simultaneous movement on both the upstream and downstream parts of the blockage would still leave a section of the blockage intact and above lake level. Retrogressive analysis of this remaining section, using the same assumptions that were used for static conditions, suggests that after a series of three successive, highly mobile failures on both sides of the blockage, the crest would be lowered below lake level and the lake could be released. The same results occur when retrogressive analysis is conducted on the section remaining after an earthquake near magnitude 6.0.

Model analysis predicts that some part of the blockage would remain intact and above lake level for all positions of the water table tested and for all earthquake magnitudes up to the maximum credible. Although large masses of blockage material are predicted to move, the altitude of the blockage crest would remain the same under the worst conditions analyzed—the water table at land surface level, a maximum credible earthquake, and simultaneous slippage from the crest toward the lake and from the crest toward Castle Creek along the deepest potential failure surfaces. Retrogressive failure analysis on the

remaining sections, however, predicts lake breakout in all cases.

DISPLACEMENT OF SLIDING MASSES

The preceding analyses have indicated that retrogressive slope failure could result in lake breakout for static conditions if the blockage were saturated and for dynamic forces if water levels were at their September 1983 positions or higher. As was concluded for static conditions, however, the degree of mobility required for the sliding masses during retrogressive failure is considered unlikely to occur.

The possible displacements associated with slope failure were estimated on the basis of concepts outlined by Newmark (1965). Calculations were based on the assumptions that the sliding mass moves as a coherent body and that resistance is initiated along the failure surface. An earthquake with a square acceleration pulse of 0.1–0.2-second duration and 0.5-g amplitude was assumed, the latter value corresponding to the average seismic coefficient produced by the maximum credible earthquake in the upper half of the blockage. Displacements were calculated for single pulses and for the sum of 10 pulses and are plotted against the seismic coefficient of $F_s = 1$ (fig. 24). Displacements shown in figure 24 probably overestimate actual displacement for the assumed condition, because

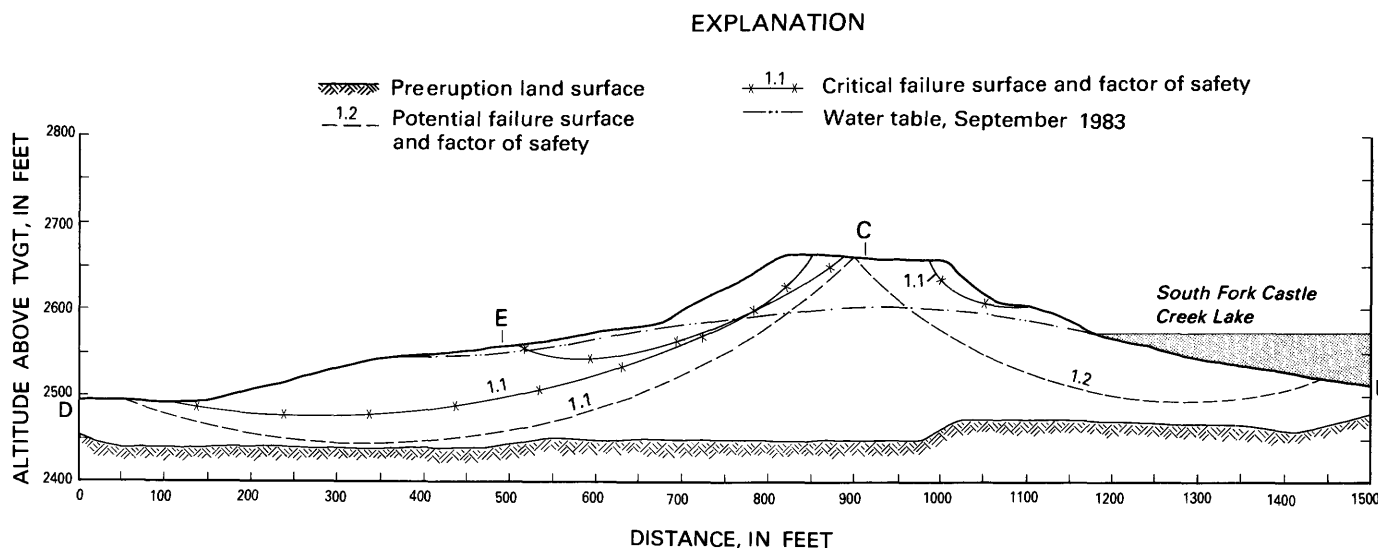


FIGURE 23.—Critical surfaces and potential failure surfaces encompassing the largest sections of the blockage for cross sections CD, CE, and CF with a seismic coefficient of 0.2 g, September 1983 water level, and zero cohesion.

pulses in opposite directions are ignored and because the value of seismic coefficients required for $F_s=1$ decreases with displacement.

Figure 16 shows values of F_s versus n_s for selected positions of the water table and can be used in conjunction with figure 24 to determine the approximate displacement of a sliding mass along a given cross section for the assumed conditions. The value n_s when F_s is equal to 1.0 can be selected from figure 16 for various positions of the water table. Such a value can then be used in figure 24 to determine an approximate displacement value for slippage along a failure surface. Slide displacements for these conditions are summarized in table 5. F_s values, and therefore seismic coefficients shown in figure 16, were obtained from model analysis that assumed drained strength and are therefore not necessarily conservative. Displacements shown in table 5 are only on the order of 5 ft or less for all cross sections assuming the September 1983 position of the water table. As a result, lake breakout from retrogressive failure following earthquake-induced slope failure is considered highly improbable.

As the water table rises to 25 ft above September 1983 levels, the analysis suggests displacements up to several tens of feet on cross sections CE and CF but less than 6 ft elsewhere. For fully saturated conditions, large displacements of sliding masses are possible at sections CE and CF, because the F_s of many trial surfaces drops well below unity even under static conditions. Such displacements cannot be estimated in the above analysis, but it is doubtful that movement would exceed 100 ft. Elsewhere, for fully saturated conditions, displacements of sliding masses of about 15 ft are

indicated for sections BB' and CD. The type of deformation expected along section DF, if the maximum credible earthquake occurred when the blockage was fully saturated, is shown in figure 25.

TABLE 5.—Estimated displacement of sliding masses for selected positions of the water table at South Fork Castle Creek blockage

Cross section	Water-table position	n_s for $F_s = 1$	Displacement, in feet	
			1 pulse	10 pulses
AA'	—Sept. 1983 level	0.31	0.1 to 0.2	0.5 to 2
BB'	—Sept. 1983 level	.23	0.1 to 0.4	1 to 4
	At land surface	.10	0.3 to 1	3 to 13
CD	—Sept. 1983 level	.22	0.1 to 0.4	1 to 4
	Sept. 1983 level plus 25 ft	.17	0.2 to 0.7	2 to 6
	At land surface	.09	0.4 to 2	4 to 15
CE	—Sept. 1983 level	.24	0.1 to 0.3	1 to 3
	Sept. 1983 level plus 25 ft	.08	0.4 to 2	4 to 17
	At land surface	<0	*(!)	*(!)
CF	—Sept. 1983 level	.20	0.1 to 0.5	1 to 5
	Sept. 1983 level plus 25 ft	.05	0.7 to 3	7 to 29
	At land surface	<0	*(!)	*(!)
GG'	—Sept. 1983	.43	0.02 to 0.1	0.2 to 1

*Unstable under static forces.

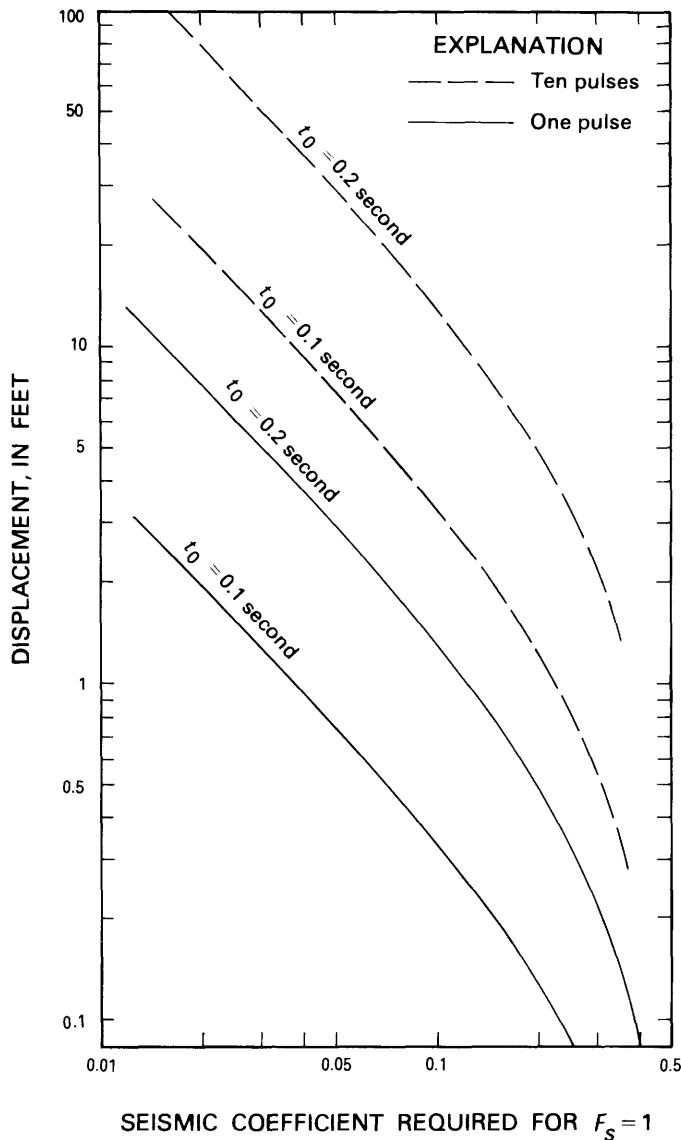


FIGURE 24.—Estimated displacement in the blockage resulting from an earthquake with an acceleration pulse of 0.5 g and duration of 0.1 and 0.2 seconds.

Seismic forces thus increase the possibility of deep-seated movements, and as ground-water levels rise, the likelihood of displacement associated with a given earthquake increases. Displacements exceeding several tens of feet are possible along sections CE and CF, either from static forces or from seismic shaking when water levels are at land surface. At other locations, however, predicted displacements are only several tens of feet or less, even for maximum credible earthquake values. The magnitude of these displacements suggests that the possibility of lake breakout, indicated by retrogressive model analysis, is remote for all positions of the water table for earthquakes equal to or less than the maximum credible earthquake for the area.

CONCLUSIONS

South Fork Castle Creek, a tributary of the North Fork Toutle River, was blocked by the debris-avalanche deposit associated with the May 18, 1980, eruption of Mount St. Helens. A lake that eventually reached a volume of 19,000 acre-ft formed behind the blockage and now poses a flood hazard of unknown magnitude to downstream areas if the blockage fails. The blockage has steep slopes and consists of unsorted and unstratified debris-avalanche deposit material that ranges from silt- and clay-sized particles to blocks tens of feet in diameter. The St. Helens seismic zone, which is believed capable of producing an earthquake larger than magnitude 5.5 but less than 7.0, passes within a few miles of the blockage. The blockage has been subjected to three historic periods of shaking, with accelerations of 0.1 or 0.2 g. These events are presumed to have caused compactions of the blockage, increasing its relative density, and should have increased the resistance of the blockage to liquefaction (Mori and others, 1978).

Unit-weight and relative-density tests suggest that the deposit at South Fork Castle Creek is moderately compacted; in this respect it is probably typical of the Mount St. Helens debris-avalanche deposit. Unfortunately, the available data are fragmentary. Further attention should therefore be given to this issue, because of its relevance to questions of liquefaction and slide mobility and to strength-pore-pressure-deformation behavior as estimated by laboratory tests on material compacted to field density.

Stability of the blockage depends heavily on ground-water conditions: as ground-water levels rise, stability of the blockage decreases. Ground-water levels were first measured in the blockage in September 1983. Depth to water below the crest of the blockage ranged from about 20 to 60 ft at that time. Water levels are believed to have been near their seasonal low in September 1983, and they could also increase annually for several more years. The potential for failure of the blockage due to gravitational forces and to horizontal forces induced by an earthquake was evaluated for water levels at their September 1983 position and higher, including saturation of the blockage. In general, results of these analyses indicate that if an earthquake with a seismic coefficient one-half that of the maximum credible occurred with water levels at their September 1983 position, substantial deformation on the blockage could occur. Slope failures could occur from the crest toward the lake and from the crest toward Castle Creek. Potential failure surfaces are deep, extending as much as 120 ft below lake level. A nearby earthquake with magnitude near 6.0 could cause much more extensive deformation on the blockage. As ground-water levels rise, the factor of safety for critical failure surfaces decreases

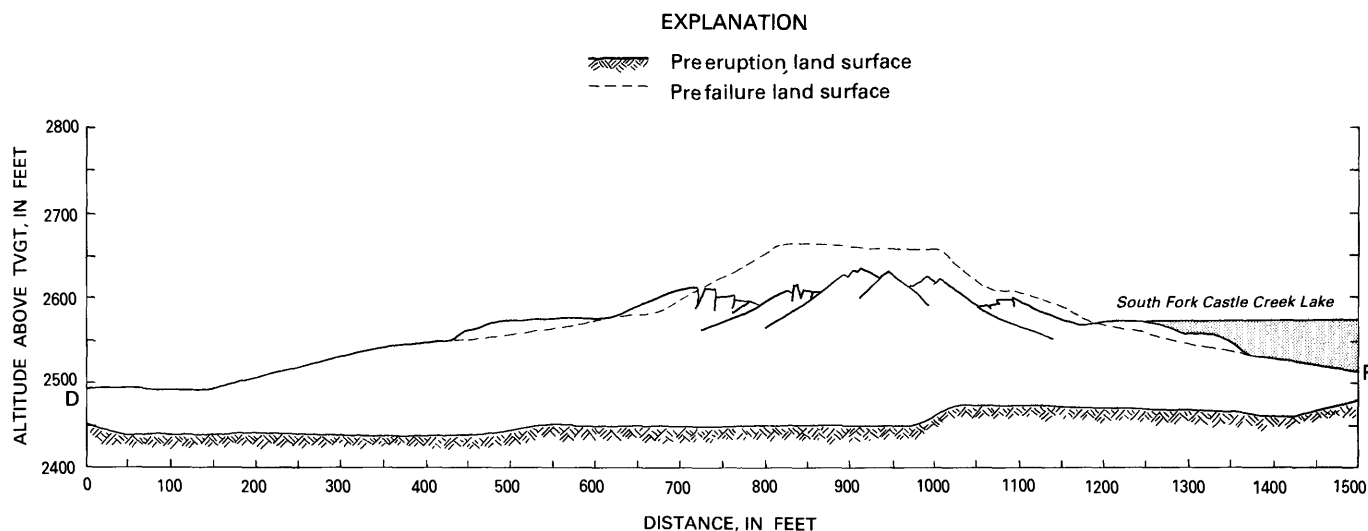


FIGURE 25.—Schematic of deformation expected with high ground-water level and maximum credible earthquake magnitude.

and potential displacement associated with a given earthquake increases. As a result, potential deformation on the blockage also increases.

Slope failure from gravitational forces presents no significant problem unless the blockage becomes nearly saturated, although some deformation of the blockage is possible at lower ground-water levels. With the blockage fully saturated, slope failures extending as much as 30 ft below lake level could occur. From the crest toward the lake and from the crest toward Castle Creek, there is a potential for deep-seated surfaces along which sliding could occur.

None of the analyses for static or dynamic slope failure indicate that immediate lake breakout would result from initial slope failure on the blockage, even if the failures occurred on both sides of the blockage simultaneously. Only when retrogressive failure is assumed using highly mobile sliding masses does the possibility of lake breakout result. For lake breakout to occur as a result of retrogressive failure, displacements along slippage faces would have to be on the order of hundreds to thousands of feet, whereas actual displacements even under the worst conditions analyzed would probably be on the order of only tens of feet.

None of the analyses indicated the potential for a breakout of South Fork Castle Creek Lake as a result of initial slope failures on the blockage, because some part of the blockage would remain intact and above lake level for all possible positions of the water table and for earthquakes up to the maximum credible magnitude for the area. Retrogressive failure in the remaining section

of the blockage could lead to lake breakout if an earthquake with a seismic coefficient in the blockage of 0.2 g occurred when ground water was at existing (September 1983) levels or higher. Retrogressive failure could also lead to lake breakout following initial slope failures induced by gravitational forces with the water table at land surface. The assumptions used in the analysis for retrogressive failures are so conservative, however, that the possibility of actual lake breakout from slope failure is considered remote.

REFERENCES

- Beaulieu, J. D., and Peterson, N. V., 1981, Seismic and volcanic hazard evaluation of the Mount St. Helens area, Washington, relative to the Trojan nuclear site, Oregon: State of Oregon Department of Geology and Mineral Industries, Open-File Report 0-81-9, 80 p.
- Grant, W. C., Weaver, C. S., Zollweg, J. E., 1984, The February 14, 1981, Elk Lake, Washington, earthquake sequence: Bulletin of the Seismological Society of America.
- Hadley, J. B., 1978, Madison Canyon rockslide, Montana, U.S.A., in Voight, Barry, ed., Rockslides and avalanches-1, Natural phenomena: Amsterdam, Elsevier Press, p. 167-180.
- Hildreth, Wes, 1983, The compositionally zoned eruption of 1912 in the Valley of Ten Thousand Smokes, Katmai National Park, Alaska: Journal of Volcanology and Geothermal Research, v. 18, p. 1-56.
- Hoblitt, R. P., Miller, C. D., and Vallance, J. W., 1981, Origin and stratigraphy of the deposit produced by the May 18 directed blast, in Lipman, P. W., and Mullineaux, D. R., eds., The 1980 eruptions of Mount St. Helens, Washington: U.S. Geological Survey Professional Paper 1250, p. 401-420.
- Jennings, M. E., Schneider, V. R., and Smith, P. E., 1981, Computer assessments of potential flood hazards from breaching of two de-

- bris dams, Toutle River, and Cowlitz River systems, *in* Lipman, P. W. and Mullineaux, D. R., eds., *The 1980 eruptions of Mount St. Helens*, Washington: U.S. Geological Survey Professional Paper 1250, p. 829-836.
- Knott, C. G., and Smith, C. M., 1980, Notes on Bandai-san: *Seismological Society of Japan Transaction*, v. 13, p. 223-257.
- Kojan, Eugene, and Hutchison, J. N., 1978, Mayunmarca rockslide and debris flows, Peru, *in* Voight, Barry, ed., *Rockslides and avalanches—1, Natural phenomena*: Amsterdam, Elsevier Press, p. 314-361.
- Lipman, P. W., 1981, Geologic map of proximal deposits and features of the 1980 eruptions, *in* Lipman, P. W., and Mullineaux, D. R., eds., *The 1980 eruptions of Mount St. Helens*, Washington: U. S. Geological Survey Professional Paper 1250, pl. 1.
- Mark, R. K., and Bonilla, M. G., 1977, Regression analysis of earthquake magnitude and surface fault length using the 1970 data of Bonilla and Buchanan: U.S. Geological Survey Open-File Report 77-614, 8 p.
- Mori, K., Seed, H. B., and Chan, C. K., 1978, Influence of sample disturbance on sand response to cyclic loading: *Journal of Geotechnical Division, American Society of Civil Engineers*, v. 104, no. GT3, p. 323-339.
- Newmark, N. M., 1965, Effects of earthquakes on dams and embankments: *Geotechnique*, v. 15, no. 2, p. 139-160.
- Plafker, George, and Ericksen, C. E., 1978, Nevados Huascaran avalanches, Peru, *in* Voight, Barry, ed., *Rockslides and avalanches—1, Natural phenomena*: Amsterdam, Elsevier Press, p. 277-314.
- Sarna-Wojcicki, A. M., Shipley, Susan, Waitt, R. B., Dzurisin, Daniel, and Wood, S. H., 1981, Areal Distribution, thickness, mass, volume, and grain size of air-fall ash from the six major eruptions of 1980, *in* Lipman, P. W., and Mullineaux, D. R., eds., *The 1980 eruptions of Mount St. Helens*, Washington: U.S. Geological Survey Professional Paper 1250, p. 577-600.
- Seed, H. B., and Martin, G. R., 1966, The seismic coefficients in earth dam design: *Journal of Soil Mechanics and Foundation Engineering Division, American Society of Civil Engineers*, no. 92, v. SM3, p. 25-28.
- Silva, Luis, Cocheme, J. J., Canul, Rene, Duffield, W. A., and Tilling, R. I., 1982, Volcanic events, El Chicon Volcano: *Scientific Event Alert Network (SEAN) Bulletin, Smithsonian Institution*, v. 7, no. 5, p. 2-6.
- Terzaghi, Karl, and Peck, R. B., 1967, *Soil mechanics in engineering practice (2d ed.)*: New York, John Wiley, 566 p.
- Trask, T. D., 1930, Mechanical analysis of sediments by centrifuge: *Economic Geology*, v. 25, p. 581-599.
- Varnes, D. J., 1978, Slope movement types and processes, *in* Schuster, R. L., and Krizek, R. J., eds., *Landslides; Analysis and control*: Washington, D.C., Transportation Research Board, p. 11-33.
- Verhoogen, John, 1937, Mt. St. Helens, a recent Cascades volcano: *Bulletin of the Department of Geological Sciences, University of California*, v. 14, no. 9, p. 2263-2309.
- Voight, Barry, 1978, Lower Gros Ventre slide, Wyoming, U.S.A., *in* Voight, Barry, ed., *Rockslides and avalanches—1, Natural phenomena*: Amsterdam, Elsevier Press, p. 113-160.
- Voight, B., Glicken, H., Janda, R. J., and Douglass, P. M., 1981, Catastrophic rockslide avalanche of May 18, *in* Lipman, P. W., and Mullineaux, D. R., eds., *The 1980 eruptions of Mount St. Helens*, Washington: U.S. Geological Survey Professional Paper 1250, p. 347-377.
- Waitt, R. B., Jr., 1981, Devastating pyroclastic density flow and attendant airfall of May 18—Stratigraphy and sedimentology of deposits, *in* Lipman, P. W., and Mullineaux, D. R., eds., *The 1980 eruptions of Mount St. Helens*, Washington: U.S. Geological Survey Professional Paper 1250, p. 439-460.
- Weaver, C. S., and Smith, S. W., 1983, Regional tectonic and earthquake hazard implications of a crustal fault zone in southwestern Washington: *Journal of Geophysical Research*.